AES/TGP/11-29

CSEM modeling of a VTI layered medium with the effective anisotropic medium

August 2011

Jide Nosakare Ogunbo

TU Delft

Department of Geotechnology

Delft University of Technology

Title	:	CSEM modeling of a VTI layered medium with the effective anisotropic medium
Author(s)	:	Jide Nosakare Ogunbo
Date	:	August 2011
Professor(s)	:	dr.Ir E.C. Slob
Supervisor(s)	:	dr.Ir E.C. Slob prof.dr.Ir. W. Mulder
TA Report number	:	AES/TGP/11-29

Postal Address	:	Section for Earth Sciences Department of Applied Earth Sciences Delft University of Technology P.O. Box 5028 The Netherlands
Telephone	:	(31) 15 2781328 (secretary)
Telefax	:	(31) 15 2781189
Electronic mail	:	nosajide@yahoo.com

Copyright ©2011 Section for Applied Geophysics and Petrophysics
All rights reserved.
No parts of this publication may be reproduced,
Stored in a retrieval system, or transmitted,
In any form or by any means, electronic,
Mechanical, photocopying, recording, or otherwise,
Without the prior written permission of the
Section for Applied Geophysics and Petrophysics

CSEM modeling of a VTI layered medium with the effective anisotropic medium

Master of Science Thesis

A thesis submitted to the Department of Geotechnology at Delft University of Tecnology in partial fulfillment of the requirements for the degree of Master of Science in Applied Geophysics

Jide Nosakare Ogunbo

August 29, 2011

Delft University of Technology Department of Geotechnology

Abstract

The numerical modeling with the diffusive controlled source electromagnetic (CSEM) method has been used to validate the published results of Ellis *et al.* (2010a) by first investigating the validity of effective medium theory for both horizontally layered isotropic and vertically transverse isotropic (VTI) layered earth. Ellis *et al.* (2010a) used 'moving window average method' to calculate bulk vertical and horizontal resistivities of resistivity logs, from which they calculated effective anisotropic ratio. The question is if the application of their local averaging scheme is valid also for a layered earth. The investigation of effective medium theory is done in horizontal wavenumber-frequency domain ($k-\omega$) which allows us to evaluate the influence of propagation and attenuation parts of the complex vertical wavenumber on the existence and stability of the effective solution for the whole range of wavenumber, k.

For the layered models considered, the total thickness is held constant while the number of layers is varied with consequent changes in thickness of the individual layer. Also, reflection and transmission interactions are both ignored and included. For the horizontally layered isotropic earth, with only propagation-diffusion term, a stable effective transverse electric (TE-mode) isotropic conductivity exists from 0.5% of maximum wavenumber irrespective of the unit thickness of a layer. But with the inclusion of reflection and transmission interactions, the effective skin depth or wavelength has to be sufficiently large compared with unit thickness of the layered earth for a stable solution to exist at all values of wavenumber, k. It is noted that effective transverse magnetic (TM-mode) isotropic conductivity is not the same as that of TE-mode for large wavenumber, k, because of the different limits of their reflection coefficients at large k.

However, there are no effective vertically transverse isotropic (VTI) parameters which satisfy the horizontally layered isotropic or VTI layered earth because the effective VTI parameters are wavenumber, k-dependent, though with approximately constant effective anisotropic ratio. We conclude that the effective medium theory adopted by Ellis *et al.*

(2010a) is not a valid approach for modeling a layered earth, though it may be valid for a local measurement.

Table of Contents

List of Figures

List of Tables

Acknowledgments

I acknowledge the help, strength and favor of the Almighty God of our Lord Jesus Christ during this thesis work. May His name be glorified.

I am indebted to Shell and Statoil for the scholarship award given to me to participate in the IDEA League Joint Master's in Applied Geophysics programme. I would like to express my profound gratitude to my supervisors dr.ir. Evert Slob and prof.dr.ir Wim Mulder for their immense support, continued encouragement and mentorial role during this project. It was indeed a great opportunity to work with them.

I am equally thankful to all my lecturers at Delft University of Technology, ETH Zurich and RWTH Aachen for their efforts and time to tutor and advise me. I had some valuable moments with Jürg Hunziker who helped out with some programming codes and for which I am grateful.

My thesis at the Delft University of Technology afforded me the privilege to meet with Hyacinth Nwosu, Jonathan Johnson, Karel van Dalen and Mattia Miorali who supported me in the best way they could; thank you guys for being there to help.

Delft, University of Technology — Jide Nosakare Ogunbo
August 29, 2011

Chapter 1

Introduction

1-1 Motivation

The motivation for this thesis is the result in the first break technical article written by Ellis *et al.* (2010a). They observed that electrical resistivity values (inverse of conductivities) inferred from the controlled source electromagnetic (CSEM) data are greater than those measured by well logs (conventional borehole electrical resistivity logs) at the same location. They attributed this difference to electrical anisotropy because the two methods used, inline CSEM and borehole logs in undeviated well, basically measure vertical and horizontal resistivities respectively. They also reported that the two other causes of electrical anisotropy are: thin layering and grain alignment. Whereas the thin layering contributes little to anisotropy, they used an effective medium model to establish that grain alignment accounts for a significant proportion of the electrical anisotropy in fine sediments such as clays and shales. In their resulting presentations, however, they fitted two model curves to the data distribution and extrapolated in the regions where there were no data. We would like to validate these results by first investigating effective medium theory.

1-2 Effective Medium theories

A representation of highly heterogeneous subsurface by an accurate effective homogeneous medium under the quasi-static limit condition is a very useful simplification of underdetermined geophysical problems (Maldovan *et al.*, 2003, Sen & Stoffa, 1995). Hoversten *et al.* (2006) noted that effective medium can be used to normalize electromagnetic data acquired in a region.

There are several effective medium theories that exist in the literature. Choy (1999) gave a thorough review of Clausius-Mossotti, Maxwell-Garnett and the Bruggeman effective theories and they are summarized thus: the Clausius-Mossotti effective theory relates macroscopic property (e.g. the dielectric constant ϵ) to a microscopic property (e.g. the molecular polarisability α) which has to be found by full quantum mechanics. The Maxwell-Garnett effective medium theory assumes a convenient model for the microscopic polarisability α for an inclusion in a host and hence it is an extension of the Clausius-Mossotti relation to arbitrary composite systems. However, with Maxwell-Garnett theory, a composite system is an asymmetric system of the inclusion and the host, hence the Maxwell-Garnett theory works only when the inclusions are of insignificant percentage of the composite system. Bruggeman effective theory finds an approximation which treats both the inclusions and host in a symmetric manner.

The Hashin-Shtrikman upper and lower bounds, **(HS)**-bounds, (Hashin & Shtrikman, 1962), are the standard reference bounds for effective parameter of macroscopically homogeneous and isotropic multiphase materials. Differential effective-medium (DEM) theory generates several realizations (iterations) from the inclusion of less stiff phase into the matrix of the stiff phase and vice versa to predict the **HS**-bounds of the effective parameters (Norris, 1985). Therefore, Sheng (1990) proposed a three-component DEM theory in which solid grains are consolidated through the presence of third component-cement material to model the electrical and elastic properties of sedimentary rocks within a unified framework. Backus (1962) derived the conditions on the elastic coefficients under which an effective medium can approximate a horizontally layered isotropic medium.

Hashin & Shtrikman (1962) considered only physical property and volume fractions of various phases of a medium to define their effective property which can fall between the **HS**-bounds. Inclusion of geometrical details of how the phases are arranged relative to each other will predict more precise effective property (Mavko *et al.*, 2003). Spherically shaped inclusions can only restrict the models to finding effective isotropic parameters (Zimmerman, 1991), however, to account for electrical anisotropy in porous rocks and sediment Ellis *et al.* (2010b) used ellipsoidal inclusions of aspect ratio less than one.

In this report we investigate the effective medium theory for layered earth models using CSEM methods in the horizontal wavenumber-frequency ($k - \omega$) domain . Two scenarios will be considered: the first scenario is for isotropic layers while the second scenario is for vertically transverse isotropic (VTI) layers. Conductivities distributed in the layers will represent the material properties; and the volume fractions are the fractional thicknesses of the layers. The additional factors we consider are the interactions at the boundaries between layers in terms of reflection, transmission and multiple reflections of the electromagnetic energy. In this thesis we address the questions of how an effective medium model can be built based on propagation-diffusion through a layered medium, and what the effect of reflection and transmission interactions between the thin layers have on this effective medium model. We use our numerical results to validate the experimental results of Ellis *et al.* (2010a).

1-3 Outline of this thesis

The remainder of this chapter will be used to define basic notations and integral transformations (space and time Fourier transformations). In the last part of this chapter the basic theories will be discussed and these will cover: Maxwell's electromagnetic wave equations decomposed into transverse electric and magnetic fields; vertical transverse isotropy (VTI); the different components of the electric and magnetic fields in the Green's tensors in a homogeneous medium and principles of Controlled Source Electromagnetic (CSEM). Chapter two is centered on evaluating the effective isotropic and VTI parameters of layered systems in transmission mode when reflection interactions are ignored. Chapter three deals with the case when the reflection and transmission interactions are included in the total electric field propagation. In chapter four, the horizontal electric field by horizontal electric dipole will be used to invert the effective medium parameters. In chapter five the results are discussed and conclusions are given.

1-4 Fundamental notations and definitions

Generally, we represent a vectorial quantity with a boldfaced letter. For example, the position vector is denoted $\mathbf{x} = x_n\mathbf{i}_n$, where the repeated lower case subscripts notation (Einstein convention) represents summation over all possible values of the index. Thus,

$$x_n\mathbf{i}_n = \sum_{n=1}^{3} x_n\mathbf{i}_n, \tag{1-1}$$

where $\mathbf{i}_n$ denotes the unit basis vectors of the right-handed Cartesian reference frame, with $n = 1, 2, 3$. In the Einstein convention, Latin subscripts take on the values $\{1, 2, 3\}$, representing vector directions along the three coordinates in space $\{x_1, x_2, x_3\}$. Greek subscripts take on values {1,2} to represent vector directions along the horizontal coordinates only. We use ∂_i to denote partial spatial differentiation with respect to coordinate x_i. Similarly, for time coordinate, t, the partial temporal differentiation is ∂_t.

1-5 Fourier transformations

Fourier transformations are used to reduce partial derivatives to algebraic numbers in the electromagnetic problem of a vertically transverse isotropic (VTI) medium. This is possible when the properties of the medium are shift invariant in time and/or in one or more spatial coordinates (de Hoop, 1995).

1-5-1 Temporal and spatial Fourier transformations

The temporal Fourier transformation of an electric field $\mathbf{E}(\mathbf{x},t)$ from space-time domain to space-frequency domain is defined as:

$$\hat{\mathbf{E}}(\mathbf{x},\omega) = \mathbf{E}(\mathbf{x},t)\int_{-\infty}^{\infty}\exp(-\mathrm{i}\omega t)dt, \tag{1-2}$$

and its inverse as

$$\mathbf{E}(\mathbf{x},t) = \frac{1}{2\pi}\hat{\mathbf{E}}(\mathbf{x},\omega)\int_{\infty}^{\infty}\exp(\mathrm{i}\omega t)dt, \tag{1-3}$$

where $\omega = 2\pi\mathrm{f}$ is the angular frequency in $(rads^{-1})$; f is the natural frequency in Hertz, the imaginary unit $\mathrm{i} = \sqrt{-1}$

In a horizontally layered VTI earth model the parameters of the medium are piecewise constant only along a reference axis, say vertical, z, axis, (Slob *et al.*, 2011). And because of the shift invariance property in the horizontal plane (x,y), two dimensional spatial Fourier transformation on time-Fourier transformed electric field $\hat{\mathbf{E}}(\mathbf{x},\omega)$ is easily done:

$$\tilde{\mathbf{E}}(\mathbf{k}_T,z,\omega) = \int_{\mathbf{x}_T=-\infty}^{\infty}\hat{\mathbf{E}}(\mathbf{x},\omega)\exp(-\mathrm{i}k_\alpha x_\alpha)d^2\mathbf{x}_T, \tag{1-4}$$

where the subscript $_T$ denotes the horizontal vector and k_α denotes the two components of the horizontal wavenumber vector.

Inverse Fourier transformation of equation (1-4) is:

$$\hat{\mathbf{E}}(\mathbf{x}_T,z,\omega) = \frac{1}{4\pi^2}\int_{-\infty}^{\infty}\tilde{\mathbf{E}}(\mathbf{k}_T,z,\omega)\exp(\mathrm{i}k_\alpha x_\alpha)d^2\mathbf{k}_T, \tag{1-5}$$

The Fourier transformation on a partial derivative of a function with respect to a spatial coordinate, x is $\mathscr{F}^t\{\partial_x\} = -\mathrm{i}k_x$ provided the function is bounded and its value tends to zero at an infinite limit of the argument.

1-5-2 Levi-Civita tensor

The Levi-Civita symbol ϵ_{ijk} will be used for the cross product. In three dimensions, the ϵ_{ijk} is:

$$\epsilon_{ijk} = \frac{(j-i)(k-i)(k-j)}{2} = \frac{(i-j)(j-k)(k-i)}{2}, \tag{1-6}$$

From (1-6),

$$\epsilon_{ijk} = \begin{cases} 1 & \text{for even permutation,} \\ -1 & \text{for odd permutation,} \\ 0 & \text{for repeated index}i{=}j \text{ or } j{=}k \text{ or } k{=}i. \end{cases} \tag{1-7}$$

For cross product:

$$(\mathbf{a}\times\mathbf{b})_j = \epsilon_{jkl}a_k b_l = a_k b_l - a_l b_k. \tag{1-8}$$

Kronecker delta is by definition:

$$\delta_{jk} = \begin{cases} 1 & \text{for j=k} \\ 0 & \text{for j} \neq \text{k.} \end{cases} \tag{1-9}$$

Using the 3D Kronecker delta properties $\delta_{jk} = \delta_{kj}$; $\delta_{jj} = 3$ and $\delta_{jk}\delta_{kl} = \delta_{jl}$

$$\epsilon_{ijk}\epsilon_{imn} = (\delta_{jm}\delta_{kn} - \delta_{km}\delta_{jn}); \quad \epsilon_{ijk}\epsilon_{ijn} = (\delta_{jj}\delta_{kn} - \delta_{kj}\delta_{jn}) = 2\delta_{kn}; \quad 2\delta_{kk} = 6$$

1-6 Theory

1-6-1 Electromagnetic wave equations

Maxwell's equations

The complete behaviour of the electromagnetic wave, in space-time $(\mathbf{x}, t)$ domain, in a medium can be deduced from the four Maxwell equations:

$$\nabla \times \mathbf{E}(\mathbf{x},t) + \mu\partial_t \mathbf{H}(\mathbf{x},t) = -\mathbf{J}^m(\mathbf{x},t), \tag{1-10}$$

$$-\nabla \times \mathbf{H}(\mathbf{x},t) + (\sigma(\mathbf{x}) + \varepsilon(\mathbf{x})\partial_t)\mathbf{E}(\mathbf{x},t) = -\mathbf{J}^e(\mathbf{x},t), \tag{1-11}$$

$$\nabla \cdot \mathbf{D}(\mathbf{x},t) = \rho(\mathbf{x},t), \tag{1-12}$$

$$\nabla \cdot \mathbf{B}(\mathbf{x},t) = 0, \tag{1-13}$$

where the constitutive relations, $\mathbf{D} = \varepsilon\mathbf{E}$ and $\mathbf{B} = \mu\mathbf{H}$ hold; σ=conductivity (S/m); ε=permittivity of the medium (F/m); μ=permeability of the medium (H/m); $\mathbf{E}$= Electric field (V/m); $\mathbf{H}$= Magnetic field (A/m); $\mathbf{B}$= Magnetic flux (T); $\mathbf{J}^m$=magnetic current (A/m^2); $\mathbf{J}^e$=electric current (A/m^2); $\mathbf{D}$=Displacement current (C/m^2)

Transforming equations (1-10) and (1-11) into space-frequency domain using the transform:

$$\nabla \times \hat{\mathbf{E}}(\mathbf{x},s) + \zeta(\mathbf{x},s)\hat{\mathbf{H}}(\mathbf{x},s) = -\hat{\mathbf{J}}^m(\mathbf{x},s), \tag{1-14}$$

$$-\nabla \times \hat{\mathbf{H}}(\mathbf{x},s) + \eta(\mathbf{x},s)\hat{\mathbf{E}}(\mathbf{x},s) = -\hat{\mathbf{J}}^e(\mathbf{x},s), \tag{1-15}$$

where $\zeta(\mathbf{x},s) = s\mu$; and $\eta(\mathbf{x},s) = \sigma + s\varepsilon$, $s = \mathrm{i}\omega$. It is observed that if $\hat{\mathbf{E}} = \hat{\mathbf{H}}$, $\eta = -\zeta$ and $\hat{\mathbf{J}}^e = -\hat{\mathbf{J}}^m$ an equivalence principle is established which makes us obtain the same Maxwell equations. Thus, this equivalence principle allows finding solutions for magnetic field vector $\hat{\mathbf{H}}(\mathbf{x},s)$ when the solutions for the electric field vector $\hat{\mathbf{E}}(\mathbf{x},s)$ are known.

Using the curl notation defined by the Levi-Civita tensor symbol in equation (1-8) the different components of equations (1-14) and (1-15), in space-frequency domain, can be written as:

$$\epsilon_{\beta\lambda 3}\partial_\lambda \hat{E}_3 + \epsilon_{\beta 3\alpha}\partial_3 \hat{E}_\alpha + \zeta\hat{H}_\beta = -\hat{J}^m_\beta, \tag{1-16}$$

$$\epsilon_{3\lambda\beta}\partial_\lambda \hat{E}_\beta + \zeta\hat{H}_3 = -\hat{J}^m_3, \tag{1-17}$$

$$-(\epsilon_{\alpha 3\beta}\partial_3 \hat{H}_\beta + \epsilon_{\alpha\beta 3}\partial_\beta \hat{H}_3) + \eta\hat{E}_\alpha = -\hat{J}^e_\beta, \tag{1-18}$$

$$-\epsilon_{3\lambda\beta}\partial_\lambda \hat{H}_\beta + \eta\hat{E}_3 = -\hat{J}^e_3. \tag{1-19}$$

Transverse Electric and Magnetic field

The transverse electric field, TE-mode, is generated by vertical magnetic dipole source and it is the part of the electric field that is transverse to an axis of reference, z axis in our layered earth case, see equation (1-17). Here the vertical electric field does not exist. Similarly, the transverse magnetic field, TM-mode, is generated by vertical electric dipole source and it is the part of the magnetic field transverse to the z-axis, see equation (1-19). The vertical magnetic field does not exist in the TM-mode. From equations (1-16) and (1-18) it can be observed that both TM and TE-modes are excited by horizontal dipole sources. Thus with just the TE and TM-modes the whole of the electromagnetic field can be known.

Vertical Transverse Isotropy (VTI)

Electromagnetic vertical transverse isotropy (VTI) is a form of anisotropy in which the horizontal and vertical electromagnetic properties of a medium differ. This implies that isotropy exists only in the plane perpendicular to an axis of symmetry. The axis of symmetry in the layered case that will be considered in this report is the vertical z axis along which the medium parameters are piecewise constant. For horizontally layered VTI model the electromagnetic field can be decomposed into transverse electric (TE) and transverse magnetic (TM) modes (Kong, 1972) with the direction of reference being the vertical direction. Now since the vertical medium parameters, $\zeta^{(v)}$, $\eta^{(v)}$, and horizontal medium parameters, ζ, η , are distinguishable in a VTI medium and by applying Fourier transformation, on equation (1-16) to (1-19) the frequency-horizontal wavenumber domain results are:

$$
\begin{aligned}
-\epsilon_{\beta\lambda 3}\mathbf{i}k_\lambda\tilde{E}_3+\epsilon_{\beta 3\alpha}\partial_3\tilde{E}_\alpha+\zeta\tilde{H}_\beta &= -\tilde{J}^m_\beta, && \text{(1-20)}\\
-\epsilon_{3\lambda\beta}\mathbf{i}k_\lambda\tilde{E}_\beta+\zeta^{(v)}\tilde{H}_3 &= -\tilde{J}^m_3, && \text{(1-21)}\\
\epsilon_{\alpha\lambda 3}\mathbf{i}k_\lambda\tilde{H}_3-\epsilon_{\alpha 3\beta}\partial_3\tilde{H}_\beta+\eta\tilde{E}_\alpha &= -\tilde{J}^e_\alpha, && \text{(1-22)}\\
\epsilon_{3\lambda\beta}\mathbf{i}k_\lambda\tilde{H}_\beta+\eta^{(v)}\tilde{E}_3 &= -\tilde{J}^e_3. && \text{(1-23)}
\end{aligned}
$$

The expression for $\tilde{E}_\alpha$ from (1-22) is substituted into (1-20) to give:

$$
\begin{aligned}
(\eta\zeta\delta_{\beta\lambda}+\epsilon_{\beta 3\alpha}\epsilon_{\alpha 3\lambda}\partial_3\partial_3)\tilde{H}_\beta = -\eta\tilde{J}^m_\beta-\epsilon_{\beta 3\alpha}\partial_3\tilde{J}^e_\alpha+\\
\eta\epsilon_{\beta\lambda 3}\mathbf{i}k_\lambda\tilde{E}_3+\epsilon_{\beta 3\alpha}\epsilon_{\alpha\lambda 3}\mathbf{i}k_\lambda\partial_3\tilde{H}_3, \qquad \text{(1-24)}
\end{aligned}
$$

which is further simplified to:

$$
\begin{aligned}
(\eta\zeta-\partial_3\partial_3)\tilde{H}_\beta = -\eta\tilde{J}^m_\beta+\epsilon_{\beta 3\alpha}\partial_3\tilde{J}^e_\alpha+\eta\epsilon_{\beta\lambda 3}\mathbf{i}k_\lambda\tilde{E}_3+\\
\mathbf{i}k_\beta\partial_3\tilde{H}_3, \qquad \text{(1-25)}
\end{aligned}
$$

Putting the expression for $\tilde{H}_\beta$ from (1-25) into equation (1-23) we have:

$$\eta^{(v)}(\partial_3\partial_3 - \frac{\eta}{\eta^{(v)}}(k_\lambda k_\lambda + \zeta\eta^{(v)}))\tilde{E}_3 = \zeta\eta\tilde{J}^e_3 + \partial_3(\mathbf{i}k_\alpha\tilde{J}^e_\alpha - \partial_3\tilde{J}^e_3) \\ -\eta\epsilon_{3\lambda\beta}\mathbf{i}k_\lambda\tilde{J}^m_\beta, \tag{1-26}$$

noting $\epsilon_{3\beta\lambda}k_\beta k_\lambda = 0$. Using vertical wavenumber, $\Gamma^2 = \frac{\eta}{\eta^{(v)}}(\kappa^2 + \gamma^2)$, where $\kappa = \sqrt{k_1^2 + k_2^2}$ is the horizontal radial wavenumber; and $\gamma = \sqrt{\zeta\eta^{(v)}}$ is the wavenumber related to vertical conductivity and $\mathfrak{Re}(\Gamma) \geq 0$. Thus equation (1-26) becomes:

$$\eta^{(v)}(\partial_3\partial_3 - \Gamma^2)\tilde{E}_3 = \zeta\eta\tilde{J}^e_3 + \partial_3(\mathbf{i}k_\alpha\tilde{J}^e_\alpha - \partial_3\tilde{J}^e_3) \\ -\eta\epsilon_{3\lambda\beta}\mathbf{i}k_\lambda\tilde{J}^m_\beta. \tag{1-27}$$

Equation (1-27) is the wave equation for the vertical electric field strength, $\tilde{E}_3$, due to point sources within the volume. $\tilde{E}_3$ is therefore a multiple of the solution of wave field (Green's function, $\tilde{G}$) whose source is the dirac function, with the point sources as the coefficient. The modified Helmholtz equation gives the wave equation with this dirac source function:

$$(\partial_3\partial_3 - \Gamma^2)\tilde{G} = -\delta(x_3 - x^s_3), \tag{1-28}$$

where the source position is $x^s_3 = z^s$. The solution for $\tilde{G}$ is well known and given by:

$$\tilde{G}(x_3 - x^s_3) = \frac{\exp(-\Gamma|x_3 - x^s_3|)}{2\Gamma}. \tag{1-29}$$

The point sources in equation (1-27) can be defined as multiple of the dirac functions:

$$\{\tilde{J}^e_r, \tilde{J}^m_r\} = \{\hat{I}^e_r, \hat{I}^m_r\}\delta(x_3 - x^s_3). \tag{1-30}$$

This definition allows us to write the solution of $\tilde{E}_3$ in terms of $\tilde{G}(x_3 - x^s_3)$ as in:

$$\eta^{(v)}\tilde{E}_3 = (-\zeta\eta\hat{I}^e_3 - \partial_3(\mathbf{i}k_\alpha\hat{I}^e_\alpha + \partial_3\hat{I}^e_3) + \eta\epsilon_{3\alpha\beta}\mathbf{i}k_\alpha\hat{I}^m_\beta)\tilde{G}(x_3 - x^s_3).$$

Carrying out the derivatives in this equation gives:

$$\tilde{E}_3 = (\frac{\Gamma}{\eta^{(v)}}\text{sign}(x_3 - x^s_3)\mathbf{i}k_\alpha\hat{I}^e_\alpha + \frac{\eta}{\eta^{(v)}}\epsilon_{3\alpha\beta}\mathbf{i}k_\alpha\hat{I}^m_\beta \\ + \frac{\hat{I}^e_3}{\eta^{(v)}}[\Gamma^2 - \eta\zeta])\tilde{G}(x_3 - x^s_3), \tag{1-31}$$

$$\tilde{E}_3 = (\frac{\Gamma}{\eta^{(v)}}\text{sign}(x_3 - x^s_3)\mathbf{i}k_\alpha\hat{I}^e_\alpha + \frac{\eta}{\eta^{(v)}}\epsilon_{3\alpha\beta}\mathbf{i}k_\alpha\hat{I}^m_\beta \\ + \frac{\eta\hat{I}^e_3}{(\eta^{(v)})^2}[\kappa^2 + \gamma^2 - \eta^{(v)}\zeta])\tilde{G}(x_3 - x^s_3). \tag{1-32}$$

With $\gamma^2 = \eta^{(v)}\zeta$:

$$\tilde{E}_3 = (\frac{\Gamma}{\eta^{(v)}}\text{sign}(x_3 - x_3^s)\mathbf{i}k_\alpha \hat{I}_\alpha^e + \frac{\eta}{\eta^{(v)}}\epsilon_{3\alpha\beta}\mathbf{i}k_\alpha \hat{I}_\beta^m + \frac{\eta \hat{I}_3^e}{(\eta^{(v)})^2}\kappa^2)\tilde{G}(x_3 - x_3^s) - \frac{\hat{I}_3^e}{\eta^{(v)}}, \tag{1-33}$$

$$\tilde{E}_3 = X_3^{TM}\tilde{G}(x_3 - x_3^s) - \frac{\hat{I}_3^e}{\eta^{(v)}}, \tag{1-34}$$

where the source factor X_3^{TM} is:

$$X_3^{TM} = (\frac{\Gamma}{\eta^{(v)}}\text{sign}(x_3 - x_3^s)\mathbf{i}k_\alpha \hat{I}_\alpha^e + \frac{\eta}{\eta^{(v)}}\epsilon_{3\alpha\beta}\mathbf{i}k_\alpha \hat{I}_\beta^m + \frac{\eta \hat{I}_3^e}{(\eta^{(v)})^2}\kappa^2). \tag{1-35}$$

The vertical component of the magnetic field ($\tilde{H}_3$) can be found using the equivalence principle, thus:

$$\tilde{H}_3 = (\frac{\bar{\Gamma}}{\zeta^{(v)}}\text{sign}(x_3 - x_3^s)\mathbf{i}k_\alpha \hat{I}_\alpha^m - \frac{\zeta}{\zeta^{(v)}}\epsilon_{3\alpha\beta}\mathbf{i}k_\alpha \hat{I}_\beta^e + \frac{\zeta \tilde{I}_3^m}{(\zeta^{(v)})^2}\kappa^2)\tilde{\tilde{G}}(x_3 - x_3^s) - \frac{\hat{I}_3^m}{\zeta^{(v)}}, \tag{1-36}$$

$$\tilde{H}_3 = X_3^{TE}\tilde{\tilde{G}}(x_3 - x_3^s) - \frac{\hat{I}_3^m}{\zeta^{(v)}}. \tag{1-37}$$

$$X_3^{TE} = (\frac{\bar{\Gamma}}{\zeta^{(v)}}\text{sign}(x_3 - x_3^s)\mathbf{i}k_\alpha \hat{I}_\alpha^m + \frac{\zeta}{\zeta^{(v)}}\epsilon_{3\alpha\beta}\mathbf{i}k_\alpha \hat{I}_\beta^e + \frac{\zeta \hat{I}_3^m}{(\zeta^{(v)})^2}\kappa^2), \tag{1-38}$$

with the vertical wavenumber given by: $\bar{\Gamma} = \sqrt{\frac{\zeta}{\zeta^{(v)}}}\sqrt{\kappa^2 + \bar{\gamma}^2}$.

Using equation (1-18) the horizontal electric field, $\tilde{E}_\alpha$, can now be obtained in terms of the vertical electric field $\tilde{E}_3$ and vertical magnetic field $\tilde{H}_3$. By multiplying equation (1-18) by $\frac{\mathrm{i}k_\lambda \mathrm{i}k_\alpha}{\eta}$ we have

$$\mathrm{i}k_\lambda \mathrm{i}k_\alpha \tilde{E}_\alpha = -\eta^{-1}\mathrm{i}k_\lambda[\mathrm{i}k_\alpha \hat{I}_\alpha^e - \mathrm{i}k_\alpha \epsilon_{\alpha 3\beta}\partial_3 \tilde{H}_\beta], \tag{1-39}$$

where $\mathrm{i}k_\alpha \epsilon_{\alpha\lambda 3}\mathrm{i}k_\lambda \tilde{H}_3 = 0$. Substitution of $\epsilon_{\alpha 3\beta}\mathrm{i}k_\alpha H_\beta$ of equation (1-24) into (1-39), $\tilde{H}_\beta$ can be eliminated. Thus equation (1-39) reduces to:

$$\mathrm{i}k_\lambda \mathrm{i}k_\alpha \tilde{E}_\alpha = -\eta^{-1}\mathrm{i}k_\lambda[\mathrm{i}k_\alpha \hat{I}_\alpha^e - \partial_3(\eta^{(v)}\tilde{E}_3 + \hat{I}_3^e)], \tag{1-40}$$

then both sides of equation (1-21) are multiplied with $\epsilon_{\alpha\beta 3}\mathrm{i}k_\beta$ to obtain

$$\mathrm{i}k_\alpha \mathrm{i}k_\lambda \tilde{E}_\lambda - \mathrm{i}k_\lambda \mathrm{i}k_\lambda \tilde{E}_\alpha = \epsilon_{\alpha\beta 3}\mathrm{i}k_\beta(\zeta^{(v)}\tilde{H}_3 + \hat{I}_3^m). \tag{1-41}$$

Using equation (1-40) to eliminate $\mathrm{i}k_\alpha \mathrm{i}k_\lambda \tilde{E}_\lambda$ from equation (1-41) gives us the horizontal electric field, E_α:

$$\tilde{E}_\alpha = \frac{\mathrm{i}k_\alpha}{\eta\kappa^2}[\mathrm{i}k_\beta \hat{I}^e_\beta - \partial_3(\eta^{(v)}\tilde{E}_3 + \hat{I}^e_3)] + \epsilon_{\alpha\beta 3}\frac{\mathrm{i}k_\beta}{\kappa^2}(\zeta^{(v)}\tilde{H}_3 + \hat{I}^m_3). \tag{1-42}$$

Again using the equivalence principle the horizontal components of the magnetic field $\tilde{H}_\alpha$ can be obtained:

$$\tilde{H}_\alpha = \frac{\mathrm{i}k_\alpha}{\zeta\kappa^2}[\mathrm{i}k_\beta \hat{I}^m_\beta - \partial_3(\zeta^{(v)}\tilde{H}_3 + \hat{I}^m_3)] - \epsilon_{\alpha\beta 3}\frac{\mathrm{i}k_\beta}{\kappa^2}(\eta^{(v)}\tilde{E}_3 + \hat{I}^e_3). \tag{1-43}$$

Substituting equations (1-33) and (1-36) into equation (1-42), the horizontal electric field becomes:

$$\tilde{E}_\alpha = X^{ETM}_\alpha \tilde{G} + X^{ETE}_\alpha \tilde{\tilde{G}}, \tag{1-44}$$

where the TE-mode Green's function is given by:

$$\tilde{\tilde{G}}(x_3 - x^s_3) = \frac{\exp(-\bar{\Gamma}|x_3 - x^s_3|)}{2\bar{\Gamma}}, \tag{1-45}$$

The electric field related TM-mode and TE-mode horizontal source functions are given by:

$$X^{ETM}_\alpha = \frac{\mathrm{i}k_\alpha \mathrm{i}k_\beta \Gamma^2 \hat{I}^e_\beta}{\eta\kappa^2} + \frac{\mathrm{i}k_\alpha \Gamma \hat{I}^e_3 \mathrm{sign}(x_3 - x^s_3)}{\eta^{(v)}} + \frac{\mathrm{i}k_\alpha \epsilon_{3\lambda\beta}\mathrm{i}k_\lambda \Gamma \hat{I}^m_\beta \mathrm{sign}(x_3 - x^s_3)}{\kappa^2}, \tag{1-46}$$

$$X^{ETE}_\alpha = -\zeta\frac{\mathrm{i}k_\alpha \mathrm{i}k_\beta \hat{I}^e_\beta + \kappa^2 \hat{I}^e_\alpha}{\kappa^2} + \frac{\epsilon_{\alpha\lambda 3}\mathrm{i}k_\lambda \mathrm{i}k_\beta \bar{\Gamma}\hat{I}^m_\beta \mathrm{sign}(x_3 - x^s_3)}{\kappa^2} + \frac{\zeta}{\zeta^{(v)}}\epsilon_{\alpha\beta 3}\mathrm{i}k_\beta \hat{I}^m_3. \tag{1-47}$$

The electric Green's tensor can be computed from the combined fields of equations (1-33), (1-36), (1-42) and (1-43). Hence, the electric Green's tensor from electric TM and TE dipole is given by

$$\tilde{\mathbf{G}}^{ee}_{kr} = \begin{pmatrix} \frac{(\mathrm{i}k_1)^2\Gamma^2}{\eta\kappa^2} & \frac{\mathrm{i}k_1 \mathrm{i}k_2 \Gamma^2}{\eta\kappa^2} & -\frac{\mathrm{i}k_1\partial_3}{\eta^{(v)}} \\ \frac{\mathrm{i}k_1 \mathrm{i}k_2 \Gamma^2}{\eta\kappa^2} & \frac{(\mathrm{i}k_2)^2\Gamma^2}{\eta\kappa^2} & -\frac{\mathrm{i}k_2\partial_3}{\eta^{(v)}} \\ \frac{-\mathrm{i}k_1\partial_3}{\eta(v)} & \frac{-ik_2\partial_3}{\eta(v)} & -\frac{\partial_3\partial_3 - \gamma^2}{\eta^{(v)}} \end{pmatrix}\tilde{G} + \begin{pmatrix} \frac{\zeta(\mathrm{i}k_1)^2}{\kappa^2} & -\frac{\zeta \mathrm{i}k_1 \mathrm{i}k_2}{\kappa^2} & 0 \\ -\frac{\zeta \mathrm{i}k_1 \mathrm{i}k_2}{\kappa^2} & \frac{\zeta(\mathrm{i}k_1)^2}{\kappa^2} & 0 \\ 0 & 0 & 0 \end{pmatrix}\tilde{\tilde{G}}, \tag{1-48}$$

and the electric Green's tensor computed by magnetic TM and TE dipole is:

$$\tilde{\mathbf{G}}^{em}_{kr} = \begin{pmatrix} \frac{\mathrm{i}k_1 \mathrm{i}k_2 \partial_3}{\kappa^2} & -\frac{(\mathrm{i}k_1)^2\partial_3}{\kappa^2} & 0 \\ \frac{(\mathrm{i}k_2)^2\partial_3}{\kappa^2} & -\frac{\mathrm{i}k_1 \mathrm{i}k_2 \partial_3}{\kappa^2} & 0 \\ -\frac{\eta \mathrm{i}k_2}{\eta(v)} & \frac{\eta \mathrm{i}k_1}{\eta(v)} & 0 \end{pmatrix}\tilde{G} + \begin{pmatrix} -\frac{\mathrm{i}k_1 \mathrm{i}k_2 \partial_3}{\kappa^2} & -\frac{(\mathrm{i}k_2)^2\partial_3}{\kappa^2} & \frac{\zeta \mathrm{i}k_2}{\zeta^{(v)}} \\ \frac{(\mathrm{i}k_1)^2\partial_3}{\kappa^2} & \frac{\mathrm{i}k_1 \mathrm{i}k_2 \partial_3}{\kappa^2} & \frac{\zeta \mathrm{i}k_1}{\zeta^{(v)}} \\ 0 & 0 & 0 \end{pmatrix}\tilde{\tilde{G}}, \tag{1-49}$$

where the first and second superscripts on the Green's tensor respectively represent the field type and the source type and the first and second subscripts their corresponding vector-components. It can be seen that the whole electromagnetic field is known once the vertical electric and magnetic field components are known. With the equivalence principle the vertical and horizontal magnetic field can be directly found from vertical and horizontal electric field. Thus, the whole electromagnetic in the layered earth model can be known once the vertical electric field is found.

1-7 Controlled Source Electromagnetic

Controlled source electromagnetic method (CSEM) is in the diffusive limit of the electromagnetic wave spectrum with frequency range of 0.1-10 Hz. By diffusion it means the wave is able to propagate far through lossy (conductive) media at this low-frequency range and the wave velocity and attenuation (skin depth) are frequency dependent (Løseth *et al.*, 2006). Consequently, the wavelength in this limit is large which therefore makes CSEM method a good candidate for defining effective medium. In the diffusive limit of the electromagnetic wave spectrum ($\sigma >> \omega\epsilon$), the vertical wavenumber is given as:

$$\Gamma = \sqrt{\kappa^2 + \mathrm{i}\omega\mu\sigma^h}, \tag{1-50}$$

where all the variables retain their usual definitions and $\mathfrak{Re}(\Gamma) \geq 0$. From now on, we use k for horizontal wavenumber in place of κ for consistency and convenience except otherwise noted. The second term under the square root on the right hand side of equation (1-50) is the diffusion constant. Also in this diffusive limit, the wavenumber related to the vertical conductivity can be expanded

$$\gamma = \sqrt{\zeta\eta^{(v)}} = \sqrt{\mathrm{i}\omega\mu\sigma^v}, \tag{1-51}$$

$$= \pm(1+\mathrm{i})\sqrt{\frac{\omega\mu\sigma^v}{2}}, \tag{1-52}$$

$$= \pm\frac{(1+\mathrm{i})}{\delta_h}, \tag{1-53}$$

where $\sqrt{\mathrm{i}} = \pm\frac{(1+\mathrm{i})}{\sqrt{2}}$, μ is the permeability of the medium, δ_h is the horizontal skin depth related to the vertical conductivity. The skin depth (δ) is defined as the distance over which the propagating electromagnetic amplitude reduces to $1/e$ of its initial value. From equations (1-52) and (1-53), the horizontal skin depth is:

$$\delta_h = \sqrt{\frac{2}{\mu\sigma^v\omega}} \approx \frac{503}{\sqrt{\sigma^v \mathrm{f}}}, \tag{1-54}$$

where $\mu = \mu_o = 4\pi \times 10^7$ H/m for the permeability of free space and angular frequency $\omega = 2\pi\mathrm{f}$, f=frequency. Similarly, the vertical skin depth related to the horizontal conductivity is given by:

$$\delta_v \approx \frac{503}{\sqrt{\sigma^h \mathrm{f}}}. \tag{1-55}$$

Whereas an electromagnetic wavelength, λ in air is simply a function of speed of light in air, c and frequency, which is given by $\lambda = \frac{c}{\mathrm{f}}$, in a conductive medium it is a function of the skin depth given by:

$$\lambda = 2\pi\delta. \tag{1-56}$$

In a typical marine CSEM survey or Seabed Logging (SBL) (Eidesmo *et al.*, 2002), the horizontal electric dipole (HED) source, of finite length, is used to emit low-frequency (0.1-10 Hz) electromagnetic signals into the surrounding media, and the response is recorded by

a 2D array of seafloor electric and magnetic field receivers (Løseth *et al.*, 2008, Constable, 2010), see Figure 1-1. Horizontal electric dipole (HED) source is preferred to the vertical electric dipole (VED) source because both TM and TE-modes are produced with HED while VED generates only TM-mode and also the field amplitudes produced by HED are higher than those of VED (Chave & Cox, 1982).

CSEM and seismic methods are complementary hydrocarbon exploration tools. While seismic method is used to delineate the reservoir structures, stratigraphy and the lateral extent, CSEM method can distinguish between reservoir fluids because of the high resistivity contrasts - usually one to three orders of magnitude apart - between saline reservoir water and hydrocarbon (Um & Alumbaugh, 2007). This however calls for caution as resistivity contrast is not an exclusive property of fluid (hydrocarbon) but resistors in the subsurface, hence CSEM interpretation is done in connection with borehole log data (Adepelumi & Falebita, 2011, Ellingsrud *et al.*, 2002). Also, the structural resolution of CSEM is lower than that of seismic method since the CSEM fields are diffusive, while seismic fields are wave fields. Furthermore, CSEM is a tool of choice in hydrocarbon exploration over magnetotelluric method because it is sensitive to both horizontal and vertical conductivity of thin resistive layer (hydrocarbon reservoir) whereas magnetotelluric method is sensitive to only horizontal conductivity (Um & Alumbaugh, 2007). The amplitude and

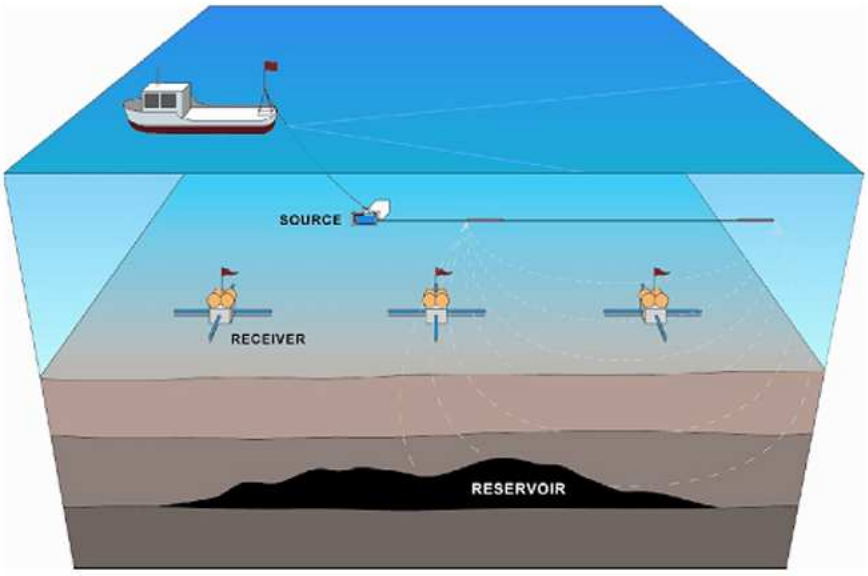

Figure 1-1: A typical marine CSEM survey layout. Towed HED source emit low frequency signal which is recorded by the seafloor electric and magnetic field receivers (From Ikelle & Amundsen (2005))

phase behaviour of an electromagnetic signal as a function of both source-receiver offset and frequency is shown in Figure 1-2(a) to 1-2(d). The x-component of the electric field from an x-directed electric source, E_{xx}, is computed with the halfspace explicit code in

(Slob *et al.*, 2010). A two halfspaces model is considered; the upper halfspace is air and it is separated from the conductive lower isotropic halfspace (water of 3 S/m conductivity) at depth $z = 0$ by an interface. The maximum positive horizontal source-receiver offset used is 10 km. In Figure 1-2(a), the source is located 960 m in the lower halfspace and receivers at 1000 m while in Figure 1-2(c), the source is 160 m deep while receivers are at 200 m depth. Operational frequencies used are 0.1, 0.4, 1.6 and 6.4 Hz. The field amplitude decays at different rates as the source-receiver offset increases. The decay is strongest in the near offset range and weakest at the far offset range. A phase change marks the beginning of airwave dominance. It can be seen that the airwave dominates the near offset receivers for the case where the source and receivers are not deeply buried (2 km for 0.4 Hz, see Figure 1-2(d)), while it dominates the far offset receivers in the case where the source and the receivers are buried deep in the lower halfspace (4 km for 0.4 Hz, see Figure 1-2(b)). Beyond this offset range the phase remains constant. In addition the airwave dominance starts earlier for higher frequencies because of the small skin depth which leads to higher attenuation of the signal that makes it fall below the noise level in the near offset range. Furthermore, airwave amplitude is lower when the source and receivers are deeply buried than in shallow water because the distance traveled by airwave in the lossy conductive water is higher when the source and receivers are deeply buried within the lower halfspace.

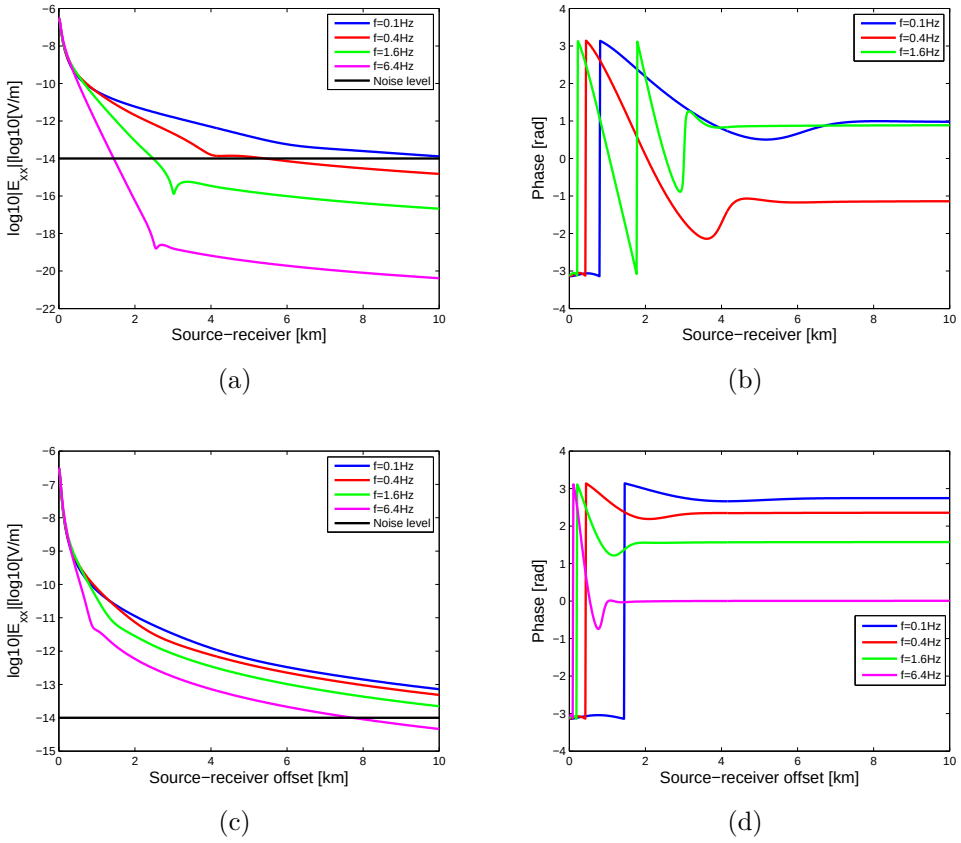

Figure 1-2: The logarithm of horizontal electric field generated by horizontal electric dipole source, E_{xx}, as a function of source-receiver offset, in homogeneous halfspace of $\sigma = 3\,\mathrm{S/m}$. In (a) source is buried at 960 m while the receivers at 1000 m and in (c) the source is buried at 160 m while the receivers at 200 m. Their respective phase plots are shown in (b) and (d)

Chapter 2

Effective conductivity parameters of layered systems in wavenumber-frequency domain

Effective conductivities (isotropic and anisotropic) of a horizontally isotropic layered system are investigated in this chapter. We model a layered earth in which each of the layers is isotropic, and invert for the effective isotropic and anisotropic parameters in the horizontal wavenumber-frequency (k-ω) domain. In the wavenumber domain the vertical wavenumber, Γ, is a complex parameter with its real part related to attenuation of the wave and the imaginary part to propagation. Thus, Γ allows for evaluating the dominance of attenuation over propagation and vice versa.

2-1 Effective conductivity in the propagation-diffusion term

In this section, we will consider only the propagation of the electric field from the source point to the receivers while neglecting the reflection and transmission interactions between the layers. The source is located on the surface, while the receivers are at the last interface of the stack of layers; this is known as the transmission mode. Except otherwise noted the model set up is: receiver spacing, $\Delta x = 4.884\,\mathrm{m}$, number of points, $N = 4096$, maximum positive horizontal source-receiver offset, $x_{max} = 10\,\mathrm{km}$ and maximum wavenumber, $k_{max} = 0.64324\,\mathrm{m}^{-1}$. Where $x_{max} = \Delta x\frac{N}{2}$, $k_{max} = \Delta k\frac{N}{2}$, $\Delta k\Delta x = \frac{2\pi}{N}$, and the range of wavenumber $k = \Delta k * i$, $(i = 1, 2, ..., \frac{N}{2})$.

The layered earth considered is shown in Figure 2-1 in which each of the layers is isotropic and conductivity values of $0.3\,\mathrm{S/m}$ and $1\,\mathrm{S/m}$ are distributed in alternating layers. This set up is similar to a resistor network which can be a series connection, when the same

current passes through all the resistors, or a parallel connection when the current flows preferentially in the direction of low resistance (Ellis *et al.*, 2010a). In the DC (direct current) limit (where angular frequency, $\omega = 0$), these resistors in series and parallel connections have resultant vertical and horizontal conductivity which are written as

$$\sigma^{v}_{eff} = T(\sum_{m=1}^{N} \frac{t_m}{\sigma_m})^{-1}, \tag{2-1}$$

for series connection; and

$$\sigma^{h}_{eff} = \frac{1}{T}\sum_{m=1}^{N} t_m\sigma_m, \tag{2-2}$$

for parallel connection. Where t_m is the thickness of the mth resistor; T is the total thickness of all N resistors in the network; σ_m is the isotropic conductivity of the individual resistor; σ^{v}_{eff} and σ^{h}_{eff} are the effective (average) vertical and horizontal conductivities. Equations (2-1) and (2-2) will be used to estimate the effective theoretical vertical and horizontal conductivities for an isotropically layered earth. In Figure 2-1 we increase the number of layers according to 2^n, where $n = 1, 2, ..., 10$, with corresponding decrease in thicknesses to keep the total thickness T of the model constant. This is to ensure that the values of the theoretical effective parameters are constant even when the number of layers changes. Unit thicknesses of odd and even layers for different number of layers are shown in Table 2-1.

Table 2-1: Unit thickness of odd (t_{odd}) and even (t_{even}) layers for different number of layers shown in Figure 2-1

No of Layers	2	4	8	16	32	64	128	256	512	1024
Unit t_{odd}(m)	800	400	200	100	50	25	12.5	6.25	3.125	1.5625
Unit t_{even}(m)	240	120	60	30	15	7.5	3.75	1.875	0.9375	0.46875

2-1-1 Effective Isotropic conductivity from TE-mode vertical wavenumber

Amplitude of the electric field propagated through an isotropically layered earth from the air-earth interface, without any loss due to reflection, to the receivers placed just below the last interface is giving as:

$$e^{-\sum_{m=1}^{N}\bar{\Gamma}_m t_m}, \tag{2-3}$$

where $\bar{\Gamma}_m$ is the TE-mode vertical wavenumber for each layer m, N is the total number of layers; t_m, the thickness of each layer. The whole stack of layers can be replaced by an effective medium with an effective medium parameter, $\bar{\Gamma}_{eff}$, such that equation (2-3) becomes:

$$e^{-\sum_{m=1}^{N}\bar{\Gamma}_m t_m} = e^{-\bar{\Gamma}_{eff}T}, \tag{2-4}$$

where $\bar{\Gamma}_{eff}$ is the effective TE-mode vertical wavenumber for the effective homogeneous and isotropic medium; T is the effective thickness of the layers. Thus TE-mode wavenumber can be used to estimate the effective isotropic conductivity, therefore from equation (2-4) we have:

$$\bar{\Gamma}_{eff} = \frac{1}{T}\sum_{m=1}^{N} \bar{\Gamma}_m t_m, \tag{2-5}$$

where, in the diffusive limit of the electromagnetic spectrum,

$$\bar{\Gamma}_m = \sqrt{k^2 + i\omega\sigma_m\mu}. \tag{2-6}$$

Similarly,

$$\bar{\Gamma}_{eff} = \sqrt{k^2 + i\omega\sigma_{eff}\mu}, \tag{2-7}$$

by putting equations (2-7) into equation (2-5), the effective isotropic conductivity, σ_{eff}, is given by:

$$\sigma_{eff} = \frac{\frac{1}{T^2}(\sum_{m=1}^{N} \bar{\Gamma}_m t_m)^2 - k^2}{i\omega\mu}. \tag{2-8}$$

Thus an effective conductivity, σ_{eff}, can be estimated for every wavenumber value, k in the range $(0 - k_{max})$. This solution is evaluated, for all the different number of layers, at constant Δx and k_{max} and at two different frequencies (0.1 and 10 Hz). Results obtained are plotted in Figure 2-2. For small wavenumber, k, where the diffusion constant dominates, at constant magnetic permeability, μ, and angular frequency, ω, the effective isotropic conductivity (from equation (2-8)) equals:

$$\sigma_{eff} = \frac{\left(\sum_{m=1}^{N} \sqrt{\sigma_m} t_m\right)^2}{T^2}. \tag{2-9}$$

For large wavenumber, k, the whole model becomes homogenized. This homogenization occurs when the squared wavenumber, $k^2 >> \omega\sigma_m\mu$, in $\bar{\Gamma}_m$ (see equation (2-6)). At this limit, $\bar{\Gamma}_m$ becomes real and the medium properties of all the layers are the same, $\bar{\Gamma}_m = k$, hence the solution is simply fractional average of the conductivity values in all the layers. This result agrees with the calculated theoretical value using equation (2-2). Thus from propagation alone anisotropy exists for small wavenumber, k range while isotropy exists for large wavenumber, k range where the effective conductivity value changes from the fractional average of the diffusion constant at zero wavenumber to the fractional average of the conductivity values at high wavenumber values. When the horizontal offset x_{max} is varied, while k_{max} remains constant, the transition value of wavenumber between anisotropy and isotropy increases as x_{max} becomes smaller than vertical offset, T. The transition value of k also increases when the frequency of transmission is increased, (from 0.1 to 10 Hz), see Figure 2-2. The reason is that at high frequency the diffusion constant of $\bar{\Gamma}_m$ is larger than the small magnitude of the wavenumber k, hence effective isotropic conductivity at this range is a function of square root of layers conductivities. The same

results are found for any number of layers at constant frequency and constant horizontal offset since interactions due to reflection are neglected.

To know the limit of k values relevant to produce useful signal we calculate effective amplitude of the TE electric field for a particular effective thickness (T) using:

$$E_{eff}^{TE} = \exp(-\bar{\Gamma}_{eff}T), \tag{2-10}$$

where $\bar{\Gamma}_{eff} = \sqrt{k^2 + \mathrm{i}\omega\mu\sigma_{eff}^{TE}}$ is the effective TE vertical wavenumber estimated from the effective TE isotropic conductivity, σ_{eff}^{TE}. In Figure 2-3 the absolute effective amplitude of the field at different wavenumber k for both 0.1 and 10 Hz for a 1 km thick layer is shown. At very small k, frequency effect (from diffusion constant of the $\bar{\Gamma}$) is more pronounced hence amplitude of the fields for 10 Hz is lower than that of 0.1 Hz due to high attenuation resulting from high frequency. For both frequencies, the amplitudes decrease from zero k to k_{max}. In this figure wavenumber-spectrum values up to 0.028 m^{-1} (4.4% of the k_{max}) produce useful signal for a 1 km thick layer. The k-values beyond this are not relevant for a 1 km thick layer because the magnitude of the effective field at these values are in the noise range ($\leq 10^{-14}$ A/m).

2-1-2 Effective Anisotropic conductivities from TM-mode vertical wavenumber

The TM-mode vertical wavenumber will be used to estimate the effective anisotropic conductivity of the model shown in Figure 2-1. In the diffusive limit, the TM-mode vertical wavenumber related to vertical conductivity is given as:

$$\Gamma = \sqrt{\frac{\sigma_h}{\sigma_v}k^2 + i\omega\sigma_h\mu}. \tag{2-11}$$

Equation (2-11) can be cast into matrix-vector form in order to invert the model parameters:

$$\mathbf{G}M = \mathbf{d}, \tag{2-12}$$

where $\mathbf{G}$ is a matrix whose row elements contain (k^2 $i\omega\mu$); M is the model parameter vector of ($\frac{\sigma_h}{\sigma_v}$ σ_h); data, $\mathbf{d}$, is $(\Gamma)^2$, where $\Gamma = \bar{\Gamma}_m$ in equation (2-6) since each layer is isotropic. Here the parameters of anisotropy are averaged over all k values, i.e. effective solutions are estimated by combining a number of wavenumber, k, to form (r by 2) $\mathbf{G}$ matrix, where $r = 2, 3, ..., n$, number of wavenumber used. This results into an overdetermined problem hence the need to use least square method for the inversion, where $G^\dagger$ is the complex conjugate transpose, the solution is:

$$M = (G^\dagger G)^{-1}G^\dagger\mathbf{d}, \tag{2-13}$$

The layered system considered is still that of Figure 2-1 and the frequency of transmission is f= 0.1 Hz and maximum positive horizontal offset, x_{max} = 2.5 km (from N = 1024

while other parameters remain constant). Effective solutions inverted are shown in Figures 2-4(a) and 2-4(b). With parameters of anisotropy averaged over the first few k, the values of both σ^h_{eff} and σ^v_{eff} increase gradually but at different rates but the layered system becomes homogeneous and isotropic as the parameter of anisotropy includes higher wavenumber, k, from $k = 0.005045\text{m}^{-1}$. Obviously, at higher average wavenumber, k, the propagation part of vertical wavenumber becomes negligible, hence effective anisotropic ratio is one. The same results are obtained for any number of layers since the reflection interactions are ignored. Figure 2-5 shows the absolute effective amplitude of the field at different wavenumber k for 0.1 Hz for a 1 km thick layer. The amplitudes decrease from zero k to k_{max}. In this figure wavenumber-spectrum values up to $0.03\,\text{m}^{-1}$ (4.7% of the k_{max}) produce useful signal for a 1 km thick layer. The k-values beyond this are not relevant for a 1 km thick layer because the magnitude of the effective field at these values are in the noise range ($\leq 10^{-14}$ A/m).

To view unique solutions of the effective horizontal and vertical conductivities, a solution space plot is made. The objective function that is minimized to find the local minima is:

$$\mathbf{f} = \frac{|\mathbf{d} - \mathbf{m}|}{\epsilon + |\mathbf{d}|}, \tag{2-14}$$

where $\mathbf{d} = (\Gamma)^2$ is the data and $\mathbf{m}$ is the model computed (from a combination of horizontal and vertical conductivity values), $\epsilon = 10^{-30}$ to stabilize the solution. Logarithm of the error function between data and model computed is shown in Figures 2-6. The solution space shows the local minima found for 2.5 km horizontal offset. These optimal local minima are found by averaging parameters of anisotropy over k values up to $0.003216\,\text{m}^{-1}$ (0.5% of k_{max}). At this value of k the optimal horizontal and vertical conductivities are not the same; thus confirming the existence of anisotropy at very small magnitude of k. However, as the parameter of anisotropy includes higher wavenumber, k, the whole set up appears homogeneous and isotropic. Solutions obtained for the different number of layers (with varying thickness values at fixed horizontal offset) are the same since the interactions at interfaces between layers are not considered.

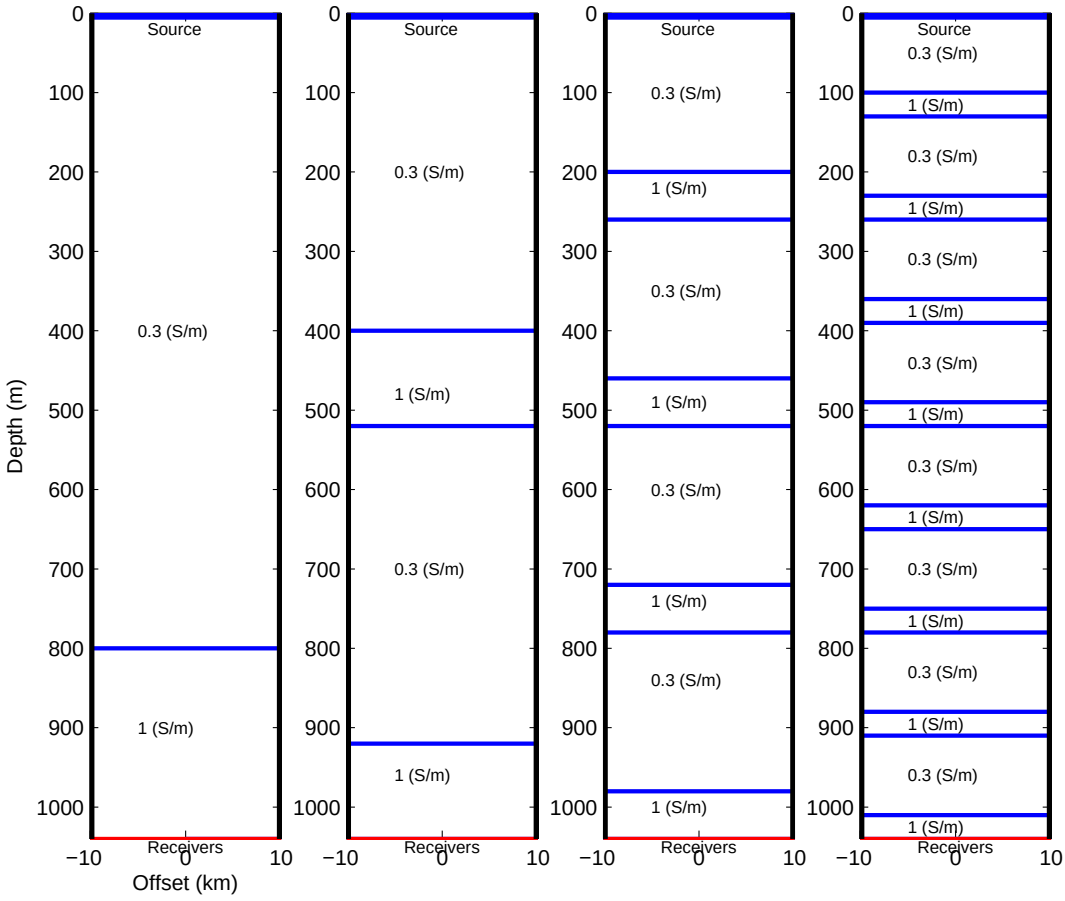

Figure 2-1: Isotropically layered earth with 0.3S/m and 1S/m distributed in alternating layers to give constant theoretical effective electrical parameters. The source is located on the surface and the array of receivers at 1040 m. While the total thickness, T, is constant, the number of layers changes according to 2^n, where $n = 1, 2, ..., 10$; only up to 16 layers are shown.

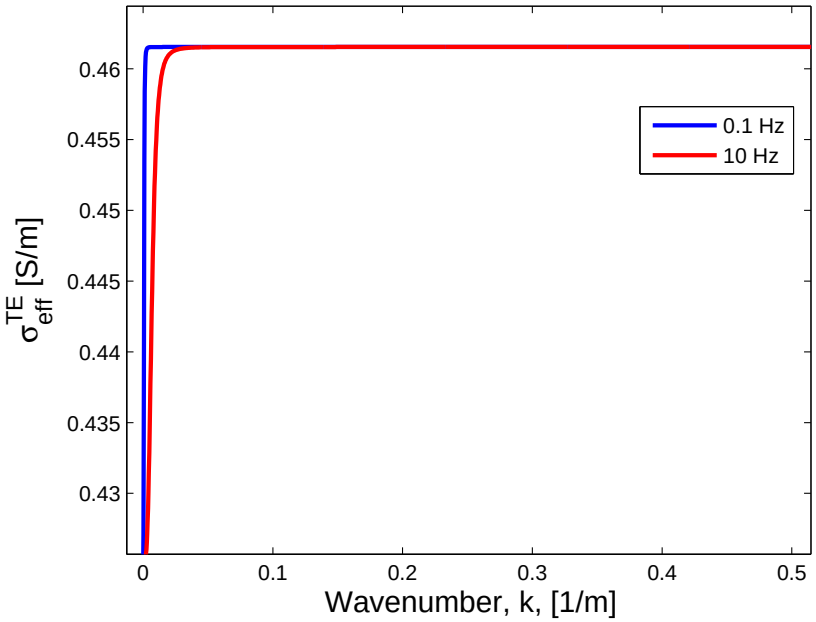

Figure 2-2: σ_{eff}^{TE} estimated at each value of wavenumber, k, for horizontally isotropic 2 layered earth when only propagation-diffusion term is considered; effective solution found at $k = 0.003458\text{m}^{-1}$ for f= 0.1 Hz and at $k = 0.03175\text{m}^{-1}$ for f= 10 Hz.

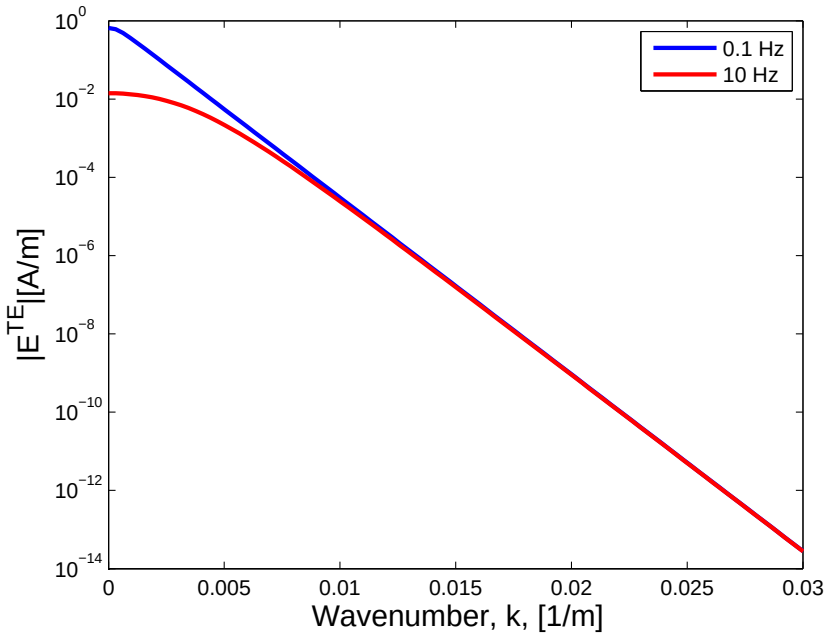

Figure 2-3: Absolute effective amplitude of TE electric field at relevant k values in the k-spectrum for 1 km thick layer at frequencies of 0.1 and 10 Hz.

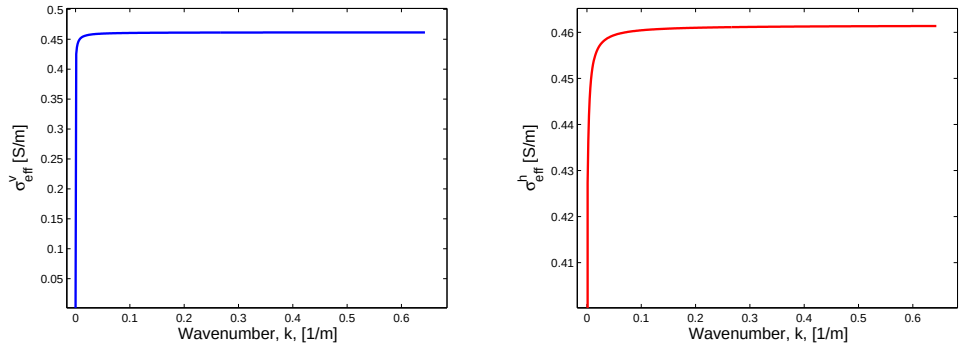

(a) (b)

Figure 2-4: Effective anisotropic parameters from TM vertical wavenumber when only propagation-diffusion term is considered: (a) shows the inverted effective vertical conductivity and (b) shows the inverted effective horizontal conductivity at different number of combination of wavenumber, k. Frequency of transmission is 0.1 Hz.

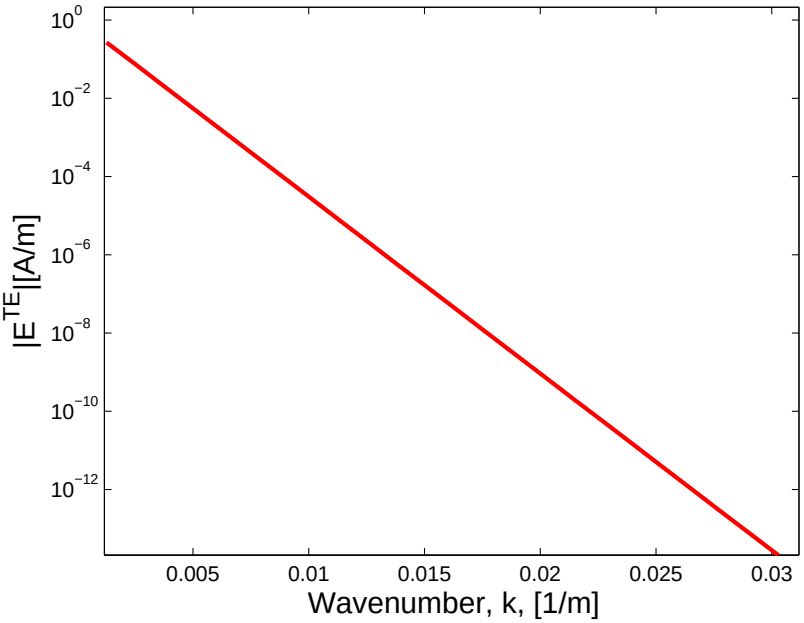

Figure 2-5: Absolute effective amplitude of TM electric field at relevant k values in the k-spectrum for 1 km thick layer at frequencies of 0.1 Hz.

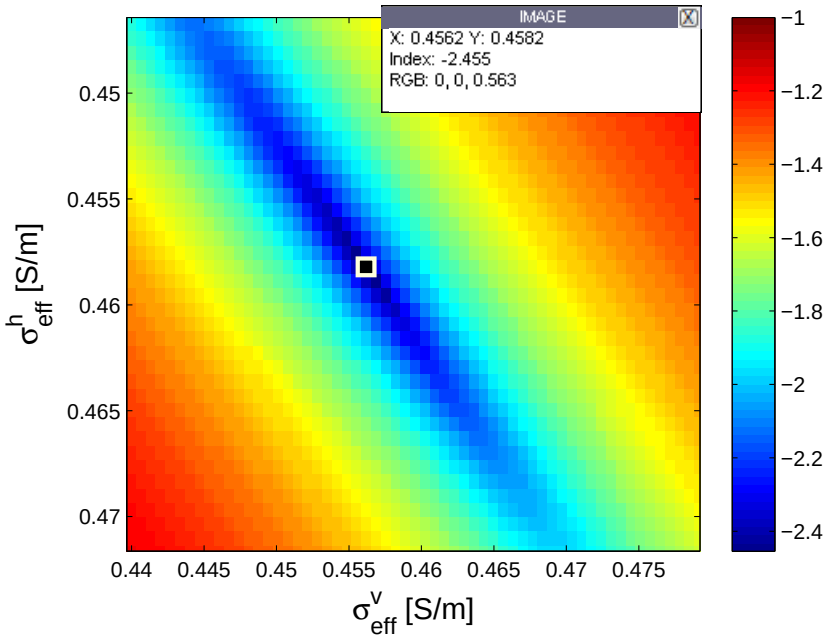

Figure 2-6: Solution space of objective function logarithm in σ^h_{eff} and σ^v_{eff} plane of a 2 layered system with conductivity distribution as shown in Figure 2-1 for 2.5 km horizontal offset.

Chapter 3

TE-mode and TM-mode effective medium parameters including thin layer reflection and transmission interactions

In this chapter the effects of reflection and transmission interactions on the effective isotropic and VTI conductivities are investigated, thereafter we consider the model with some anisotropy in each layer. We also compare the effective TE-mode isotropic conductivity of isotropically layered system with the effective TM-mode isotropic conductivity. And lastly, we use the TM-mode vertical wavenumber to find the optimal effective VTI parameters of a VTI layered earth of varying conductivity contrasts and anisotropic ratios.

3-1 Effective medium parameters from electric field due to propagation and reflection interactions

3-1-1 Boundary conditions

When an electromagnetic wave propagates through a domain $\mathbb{D}_1$, the field experiences a discontinuity in the medium properties at the interface $\mathbb{S}$ separating domains $\mathbb{D}_1$ and $\mathbb{D}_2$, see Figure 3-1. The discontinuity is due to the difference in their constitutive parameters. Boundary conditions are usually imposed to quantify fields in region $\mathbb{D}_2$ as a function of fields in regions $\mathbb{D}_1$ and to restrict the discontinuity in the field quantities to finite magnitude or zero since all physical quantities have bounded magnitudes and energy must be transferred continuously across an interface. Electromagnetic fields move from region $\mathbb{D}_1$ to $\mathbb{D}_2$ when the interface $\mathbb{S}$ is traversed along the direction of the unit vector n, which

is normal to $\mathbb{S}$. To avoid impulsive sources (Dirac) being distributed on the interface $\mathbb{S}$, two boundary conditions are given:

1. Tangential components of the electric, $\mathbf{E}$, and magnetic, $\mathbf{H}$, fields are continuous across $\mathbb{S}$

$$\mathbf{n} \times \mathbf{E} \text{ is continuous across } \mathbb{S}, \tag{3-1}$$
$$\mathbf{n} \times \mathbf{H} \text{ is continuous across } \mathbb{S}. \tag{3-2}$$

2. Normal components of the total electric current and magnetic flux density $\mathbf{B}$ are continuous across $\mathbb{S}$

$$\mathbf{n}.(\sigma + \varepsilon\partial_t)\mathbf{E} \text{ is continuous across } \mathbb{S}, \tag{3-3}$$
$$\mathbf{n}.\mathbf{B} \text{ is continuous across } \mathbb{S}. \tag{3-4}$$

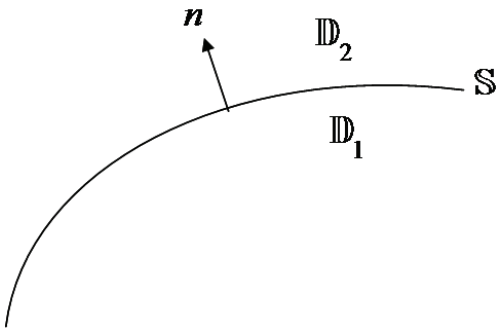

Figure 3-1: Interface $\mathbb{S}$, normal to the unit vector n, separating domains $\mathbb{D}_1$ and $\mathbb{D}_2$ of different electromagnetic properties.

3-1-2 Forward model using TE-mode field

We will use the TE-mode electric field to investigate the conditions and factors which influence the existence and stability of effective isotropic conductivity for a horizontally layered isotropic earth model when the reflection and multiple reflection interactions with the interfaces are included in the propagation of the wave field. In the layered earth model of Figure 3-2, the TE-mode electric field at any depth z can be measured. The source is located on the surface and the receivers on the last interface. Material properties, μ_n, ε_n and σ_n, are distributed in each layer of thickness d_n. Depth of interface n, from the surface is denoted as z_n. The upper halfspace is the domain $\mathbb{D}_0$, which is the air. The domain for the layered earth is $\mathbb{D}_n$, while the lower domain, $(\mathbb{D}_{N+1})$, is for the lower halfspace (basement in this example).

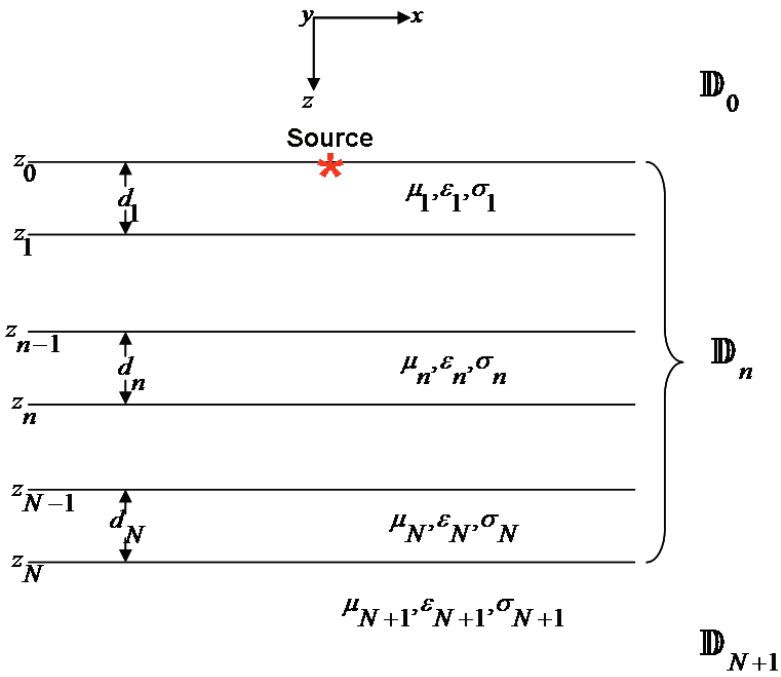

Figure 3-2: Layered earth with isotropic medium parameters $(\mu_n, \varepsilon_n, \sigma_n)$ distributed in each layer of thickness d_n in the domain $\mathbb{D}_n$. The depth to the electric interface is denoted by z_n. The upper halfspace is the air domain $\mathbb{D}_0$, and domain $\mathbb{D}_{N+1}$ is the lower halfspace with medium parameters $(\mu_{N+1}, \varepsilon_{N+1}, \sigma_{N+1})$.

The amplitude of TE-mode electric field at the air-earth interface is given:

$$E_0 = \exp(-\bar{\Gamma}_0 d^s) + \bar{R}_0 \exp(-\bar{\Gamma}_0 d_0), \tag{3-5}$$

where $d_0 = z_0$ the depth of air-earth interface usually taken as zero; d^s is the thickness between source depth and d_0. The first term on the right hand side of equation (3-5) is the direct field from source to the interface (air-earth) while the second term represents the reflected energy on the interface z_0 with $\bar{R}_0$ being the air-earth interface TE-mode global reflection coefficient. In domain $\mathbb{D}_1$, $z_0 \leq z \leq z_1$, the amplitude of the electric field at any z is a combination of the downgoing and upgoing wave energy in the domain:

$$E_1 = E_1^+ \exp(-\bar{\Gamma}_1(z - z_0)) + E_1^- \exp(-\bar{\Gamma}_1(z_1 - z)) \tag{3-6}$$

where the superscripts, minus and positive signs represent upgoing and downgoing directions respectively. With the source on the surface, E_1^- is the reflected energy of E_1^+ on the interface z_1, hence

$$E_1^- = E_1^+ \bar{R}_1 \exp(-\bar{\Gamma}_1 d_1) \tag{3-7}$$

where $d_1 = z_1 - z_0$ and $\bar{R}_1$ is the transverse electric (TE) mode global reflection coefficient at depth z_1. Now, equation (3-6) can be re-written as:

$$E_1 = E_1^+(\exp(-\bar{\Gamma}_1(z - z_0)) + \bar{R}_1 \exp(-\bar{\Gamma}_1(z_1 - z + d_1))) \tag{3-8}$$

In horizontal wavenumber domain, the boundary conditions stated in equation (3-1) to (3-4) apply only to the vertical electric field components. Therefore at $z = z_0$, after the application of boundary condition, stated in (3-1), on the true total field we have the approximation:

$$E_0^{TE}(z_o) = E_1^{TE}(z_0), \tag{3-9}$$

Putting (3-5) and (3-8) into (3-9) we have

$$E_1^{+} = \frac{1 + \bar{R}_0}{1 + \bar{R}_1 \exp(-2\bar{\Gamma}_1 d_1)}. \tag{3-10}$$

A similar derivation for electric field in domain $\mathbb{D}_n$ is possible.

Therefore at the interface z_N, the electric field, E_{N+1}^{TE}:

$$E_{N+1}^{TE} = (\prod_{m=0}^{N} \frac{(1 + \bar{R}_m)\exp(-\bar{\Gamma}_m d_m)}{(1 + \bar{R}_{m+1}\exp(-2\bar{\Gamma}_{m+1} d_{m+1}))}), \tag{3-11}$$

where $\bar{R}_m$ is the TE-mode global reflection coefficient for each layer m and it is given by a recursive equation:

$$\bar{R}_m = \frac{\bar{r}_m + \bar{R}_{m+1}\exp(-2\bar{\Gamma}_{m+1} d_{m+1})}{1 + \bar{r}_m \bar{R}_{m+1}\exp(-2\bar{\Gamma}_{m+1} d_{m+1})}, \tag{3-12}$$

where $\bar{R}_{N+1}$=0, since there is only transmission of electric field in the $N + 1$ layer. Since the magnetic permeability of the earth materials (μ) is approximately the same as the magnetic permeability in vacuum, (μ_0), the TE local reflection coefficient $\bar{r}_m$ is

$$\bar{r}_m = \frac{\bar{\Gamma}_m - \bar{\Gamma}_{m+1}}{\bar{\Gamma}_m + \bar{\Gamma}_{m+1}}, \tag{3-13}$$

where $\bar{\Gamma}_m = \sqrt{k^2 + i\omega\mu\sigma_m^h}$, in the diffusive limit of the electromagnetic wave, is the vertical wavenumber in each layer m and k is the wavenumber.

3-1-3 Effective isotropic medium for the isotropic layered earth with TE-mode

The overburden (layered earth) of Figure 3-2 can be replaced with an effective isotropic model with effective conductivity of σ_{eff} as illustrated in Figure 3-3. The total thickness, T of the overburden is held constant and the effective TE-mode electric field is:

$$E_{N+1}^{TE} = \frac{(1 + \bar{R}_{eff})(1 + \bar{R}_0)\exp(-\bar{\Gamma}_{eff} T)}{(1 + \bar{R}_{eff}\exp(-2\bar{\Gamma}_{eff} T))}, \tag{3-14}$$

where

$$\bar{R}_0 = \frac{\bar{r}_0 + \bar{R}_{eff}\exp(-2\bar{\Gamma}_{eff} T)}{1 + \bar{r}_0 \bar{R}_{eff}\exp(-2\bar{\Gamma}_{eff} T)}, \tag{3-15}$$

$$\bar{r}_0 = \frac{\bar{\Gamma}_0 - \bar{\Gamma}_{eff}}{\bar{\Gamma}_0 + \bar{\Gamma}_{eff}}, \tag{3-16}$$

$$\bar{r}_{eff} = \frac{\bar{\Gamma}_{eff} - \bar{\Gamma}_{N+1}}{\bar{\Gamma}_{eff} + \bar{\Gamma}_{N+1}}, \tag{3-17}$$

where $\bar{R}_{eff} = \bar{r}_{eff}$; $\bar{R}_{eff}$ is the global TE reflection coefficient of the interface separating the effective medium in domain $\mathbb{D}_{eff}$ and domain $\mathbb{D}_{N+1}$, $\bar{r}_{eff}$ is its local reflection coefficient; $\bar{R}_0$ is the global TE reflection coefficient of the interface between domain $\mathbb{D}_0$ and effective medium domain $\mathbb{D}_{eff}$, and $\bar{r}_0$ is its local reflection coefficient; $\bar{\Gamma}_0$ and $\bar{\Gamma}_{eff}$ are the TE vertical wavenumber for domains $\mathbb{D}_0$ and $\mathbb{D}_{eff}$ respectively.

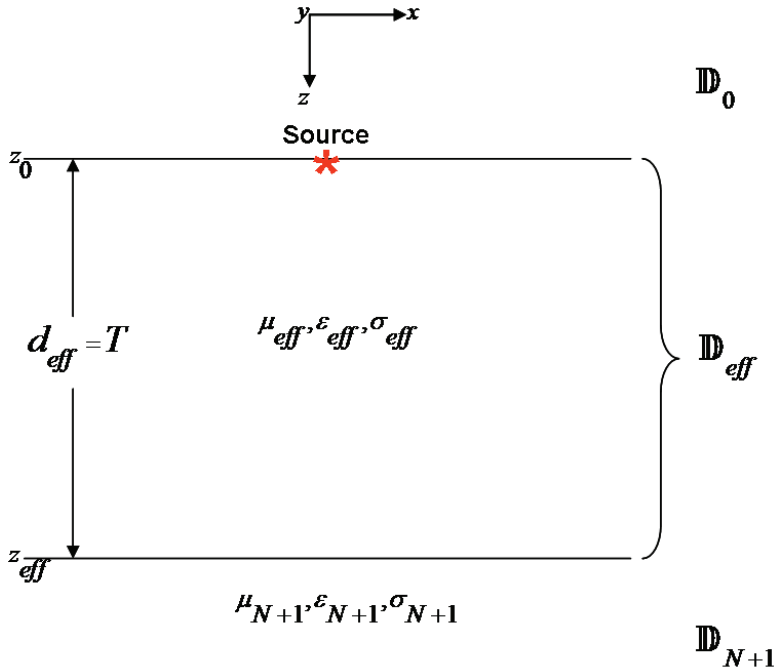

Figure 3-3: Effective medium for the model shown in Figure 3-2. $\mu_{eff}, \varepsilon_{eff}$ and σ_{eff} are the effective isotropic medium parameters, T effective thickness of the overburden

Figure 3-4 shows the set up of the model. It contains 1040 m thick overburden of sediment on the infinitely thick basement rock of conductivity, 0.02 S/m. The overburden is split into different number of layers of 2, 4, 8,..., 1024 layers while the total thickness is held constant. 0.3 S/m and 1 S/m are distributed into layers in an alternating manner. This set up is a transmission mode configuration where the source is on the surface and the receivers are located below the last interface at 1040 m depth. Unit thicknesses of odd and even layers for different number of layers are shown in Table 2-1.

Data are computed with equation (3-11) and the model with equation (3-14) at two different frequencies, f= 0.1 Hz and f= 1 Hz and at different values of k within $(0 - k_{max})$ range. The effective isotropic conductivity will be inverted by optimizing the error between the model

and the data. Number of layers (consequently the unit thicknesses) are varied in the usual sequence to investigate the influence of the reflection on the inverted effective conductivity. Data at $k = 0$ is zero in the diffusive approximation because at the air-earth interface the TE-mode local reflection coefficient is $\bar{r}_0 = -1$, which makes the global reflection in the air $\bar{R}_0$=-1. With this value substituted into equation (3-11) the whole product becomes zero. It means that this energy at $k = 0$ is not useful for inverting the effective solution. At higher k-values, the propagation part of the vertical wavenumber becomes negligible (i.e., the vertical wavenumber is no longer influenced by conductivity), hence $\bar{\Gamma}_m = k$ becomes real for all the layers. Hence, the inverted solution at this limit is a fractional average of conductivity values in all the layers, because we are in the regime where the static approximation is valid, see Figure 3-5 for plot of effective TE isotropic conductivity for 2 and 1024 layers. At very small k, the effective isotropic conductivity deviates more for number of layers with large unit thickness (as shown in Table 2-1). However, the effective solution is the same for any number of layers at high magnitude of k, see Figure 3-8(a).

Figure 3-6 shows the absolute effective amplitude of the TE electric field (using equation (2-10)) at different wavenumber k for 0.1 Hz for a 1 km thick layer. The amplitude variation with wavenumber is the same for the 2 and 1024 layers because the same frequency is used and the difference in effective conductivity even at small k is not large enough to cause a large deviation for a 1 km thick layer. The amplitude decreases from zero k to k_{max}. In this figure wavenumber-spectrum values up to $0.028\,\mathrm{m}^{-1}$ are the only relevant k values for producing useful signal for a 1 km thick layer. The k-values beyond this are not relevant for a 1 km thick layer because the magnitude of the effective field at these values are in the noise range ($\leq 10^{-14}$ A/m)

Absolute TE-mode effective multiple ($\mathbf{M}$) reflection amplitude is also shown in Figure 3-7. Where effective multiple reflection from equation (3-24) is given as:

$$\mathbf{M} = 1 + \bar{R}_{eff} \exp(-2\bar{\Gamma}_{eff} T) \tag{3-18}$$

where T is taken to be 1 km thick layer. For this 1 km the effective TE multiple reflection is approximately unity for all values of k implying that the existence and stability of effective solutions are independent of the multiple reflections.

To investigate the influence of the magnitude of conductivity contrast between adjacent layers on the effective isotropic conductivity, the usual distribution is changed. Values of the effective conductivities are changed by replacing the conductivity distribution of $(0.3 \;\; 1)\,\mathrm{S/m}$ in the model with the pairs $(0.3 \;\; 0.5)\,\mathrm{S/m}$ and $(0.3 \;\; 0.375)\,\mathrm{S/m}$ at frequency of transmission of 1 Hz. For the 25% conductivity contrast, $(0.3 \;\; 0.375)\,\mathrm{S/m}$, between adjacent layers, Figure 3-9(a) shows a stable effective conductivity of $0.3173\,\mathrm{S/m}$ for all values of k from 128 to 1024 layers. From Table 2-1, the combined unit thickness of the periodic (pair of) layers for 128 layers is $l_u = 16.25\,\mathrm{m}$ therefore ratio of effective skin depth (δ_{eff}) to l_u is $\frac{\delta_{eff}}{l_u} = 55$. Where effective skin depth is given by:

$$\delta_{eff} \approx \frac{503}{\sqrt{\sigma_{eff}\mathrm{f}}}, \tag{3-19}$$

where f= 1 Hz in our case. Figure 3-9(b) shows that for conductivity distribution of (0.3 0.5) S/m in the layers the stable effective conductivity, 0.34615 S/m, for all values of k exists from 256 to 1024 layers. For the 256 layers the ratio $\frac{\delta_{eff}}{l_u}$ is 105. Also for conductivity contrast of (0.3 1) the effective conductivity, 0.4615 S/m, exists for all values of k from 512 to 1024 layers as shown in Figure 3-8(b). The calculated $\frac{\delta_{eff}}{l_u}$ is 182.

It is thus established that as the conductivity contrast between adjacent layers increases the unit thickness in a layered system will have to be reduced with respect to the effective skin depth for the effective solution to exist at all values of k in this static limit where the effective conductivity is the fractional average of the conductivity values in all the layers. For 25% conductivity contrast (e.g., (0.3 0.375) S/m) the unit thickness is at most $\frac{1}{55}\delta_{eff}$; for 66% contrast (e.g., (0.3 0.5) S/m) the unit thickness is at most $\frac{1}{105}\delta_{eff}$ and for very high conductivity contrast (0.3 1) S/m, (about 231% contrast), the maximum unit thickness is $\frac{1}{182}\delta_{eff}$.

3-1-4 Effective isotropic medium for the isotropic layered earth with TM-mode

An isotropic layered earth can also be modeled with the TM-mode field by setting the anisotropic ratio (σ_h/σ_v) of the TM vertical wavenumber, to one. Thus it is also possible to invert effective TM isotropic conductivity which can be compared with effective TE isotropic conductivity estimated in the preceding subsection. The general TM-mode electric field recorded by receivers placed on z_N of the layered system in Figure 2-1, similar to equation (3-11), will be used to produce the data recorded by the receivers. However, the TM-mode reflection coefficient will now be used. The electric field E^{TM}_{N+1} is given by:

$$E^{TM}_{N+1} = (\prod_{m=0}^{N} \frac{(1+R_m)\exp(-\Gamma_m d_m)}{(1+R_{m+1}\exp(-2\Gamma_{m+1}d_{m+1}))}), \tag{3-20}$$

where $d_0 = 0$, and R_m is the TM-mode global reflection coefficient for each layer and it is given by an upward recursive equation:

$$R_m = \frac{r_m + R_{m+1}\exp(-2\Gamma_{m+1}d_{m+1})}{1 + r_m R_{m+1}\exp(-2\Gamma_{m+1}d_{m+1})}, \tag{3-21}$$

where R_{N+1}=0; the TM-mode local reflection coefficient r_m, in the diffusive limit, is

$$r_m = \frac{\sigma_{m+1}\Gamma_m - \sigma_m\Gamma_{m+1}}{\sigma_{m+1}\Gamma_m + \sigma_m\Gamma_{m+1}}, \tag{3-22}$$

where $\Gamma_m = \sqrt{k^2 + i\omega\mu\sigma^h_m}$, in the diffusive limit of the electromagnetic wave, is the vertical wavenumber in each layer m and k is the wavenumber.

Effective TM isotropic conductivity (σ^{TM}_{eff}) is inverted for conductivity distribution of (0.3 1) S/m in Figure 3-4 to investigate if solutions are the same with σ^{TE}_{eff} values. Figure 3-10(a)

shows the σ_{eff}^{TM} at different wavenumber k values. For all the different number of layers, σ_{eff}^{TM} is approximately the same at $k \approx 0$ but with increasing deviation as k increases and at sufficiently large k the solution becomes constant. Higher magnitude of effective solutions are found for thin layers (from 8 to 1024) than for 2 and 4 layers. A zoom in on the value of σ_{eff}^{TM} at $k \approx 0$ in Figure 3-10(b) shows that

$$\sigma_{eff}^{TM} = \sigma_{eff}^{TE} \tag{3-23}$$

The reason for the differences in σ_{eff}^{TE} and σ_{eff}^{TM} may be due to the different sensitivities of the TE and TM-modes. The other reason is that for large values of k when $\Gamma \approx k$ the TM-mode local reflection coefficient is equal to the DC electric reflection coefficient, while the local TE-mode reflection coefficient is zero for those large k values. This leads to different effective medium conductivity values between the TE-mode and TM-mode results.

Figure 3-11 shows the absolute effective TM amplitude (using equation similar to equation (2-10) but with the effective TM vertical wavenumber) of the field at different wavenumber k for 0.1 Hz for a 1 km thick layer. The amplitude variation with wavenumber is the same for all the different number of layers because even at small values of k the the differences between the effective solution for different layers are negligible. The amplitude decreases from zero k to k_{max}. In this figure, wavenumber-spectrum values up to $0.028\,\mathrm{m}^{-1}$ are the only relevant k values for producing useful signal for a 1 km thick layer. The k-values beyond this are not relevant for a 1 km thick layer because the magnitude of the effective field at these values are in the noise range ($\leq 10^{-14}$ A/m)

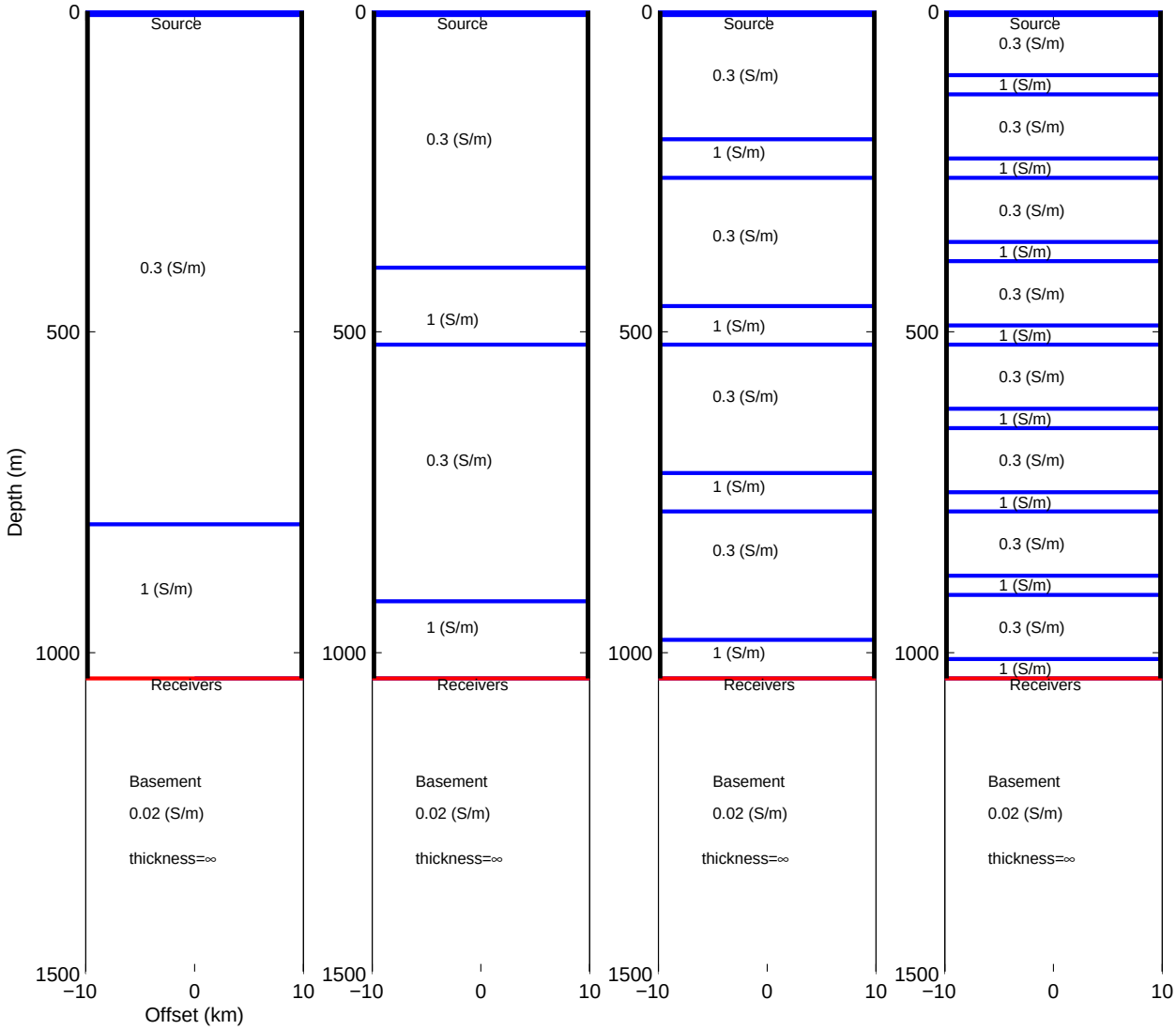

Figure 3-4: Isotropically layered overburden with 0.3 S/m and 1 S/m distributed in alternating layers to give constant theoretical effective electrical parameters. The basement is infinitely thick with conductivity of 0.02 S/m. The source is located on the surface and the array of receivers at 1040 m. While the total thickness is constant, the number of layers (from LHS to RHS) increases from 2 to 4 8 and 16 .

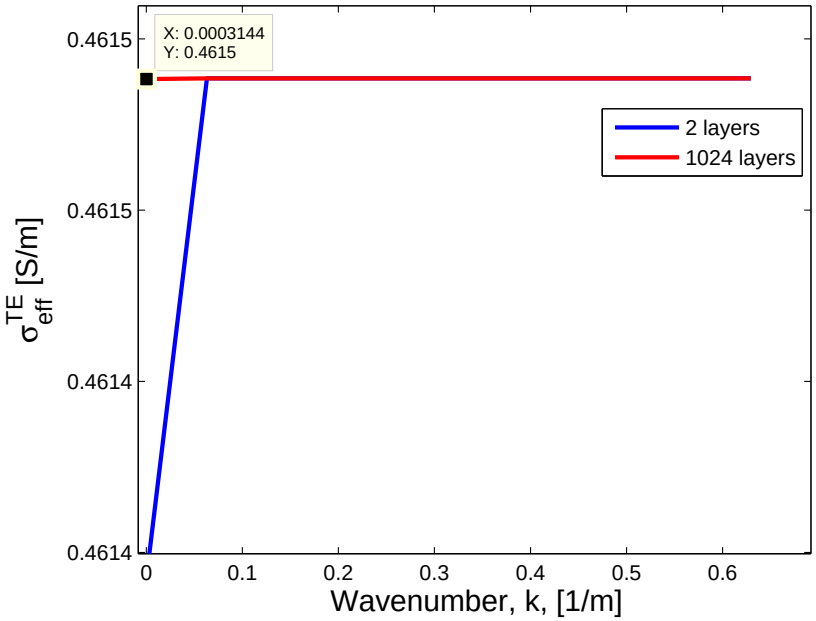

Figure 3-5: σ_{eff}^{TE} estimated as a function of wavenumber, k, for horizontally layered isotropic medium (2 and 1024 layers) with conductivity distribution of (0.3 1) in layers at f= 0.1 Hz, when the reflection and transmission interactions with layers boundaries are included.

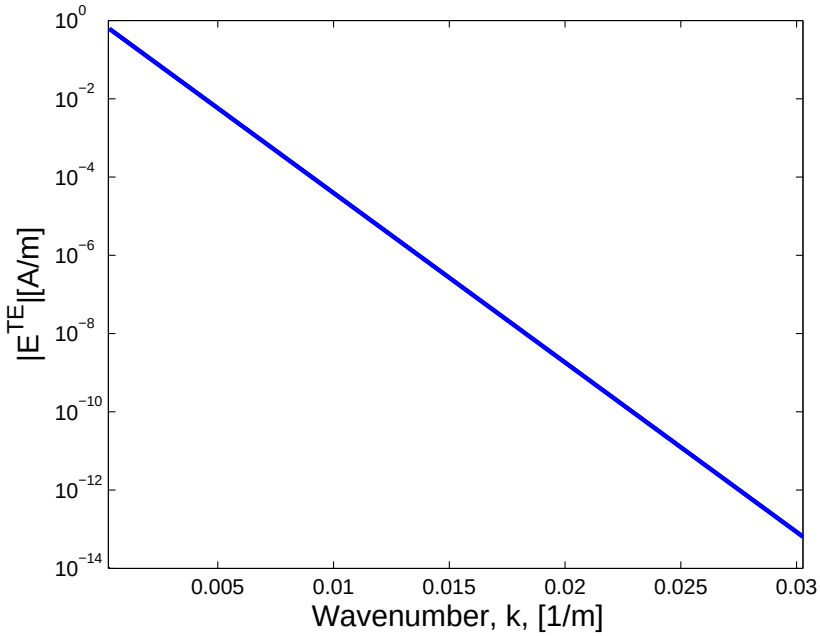

Figure 3-6: Absolute effective amplitude of TE electric field at relevant k values in the k-spectrum for 1 km thick layer at frequencies of 0.1 Hz for both 2 and 1024 layers.

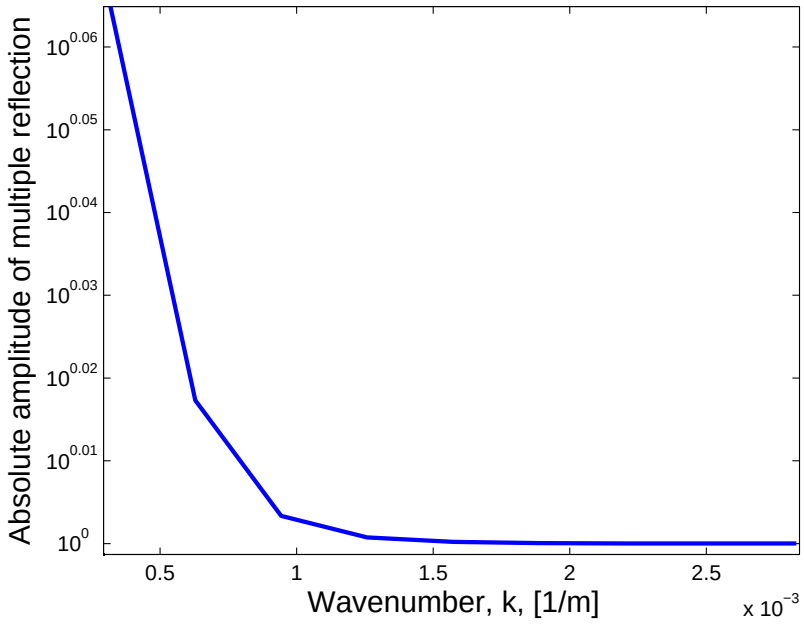

Figure 3-7: Absolute effective multiple amplitude of TE electric field at relevant k values in the k-spectrum for 1 km thick layer at frequencies of 0.1 Hz for both 2 and 1024 layers.

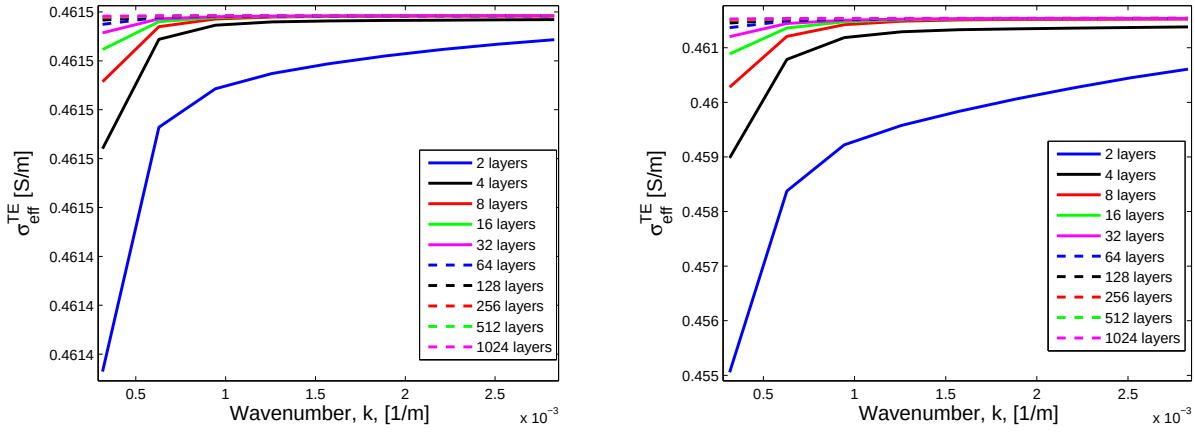

(a) (b)

Figure 3-8: Variation of σ^{TE}_{eff} at small magnitude of wavenumber, k, for different number of layers where (a) is for frequency, f= 0.1 Hz and (b) at f= 1 Hz when reflection and transmission interactions with layers boundaries are included.

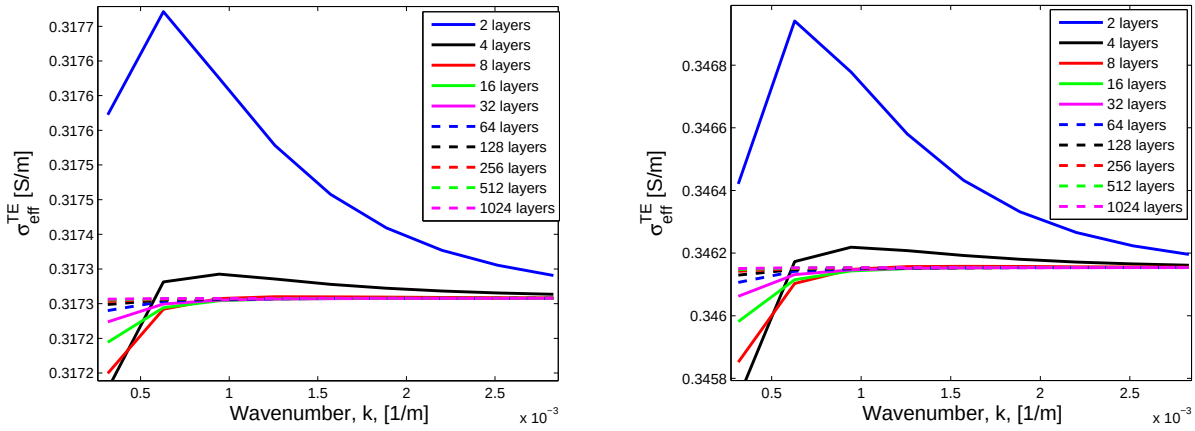

(a) (b)

Figure 3-9: σ_{eff}^{TE} estimated for all layers of different conductivity distributions, (a) (0.3 0.375), and (b) (0.3 0.5) in Figure 3-4 in the horizontally layered isotropic medium at f= 1 Hz with the inclusion of reflection and transmission interactions.

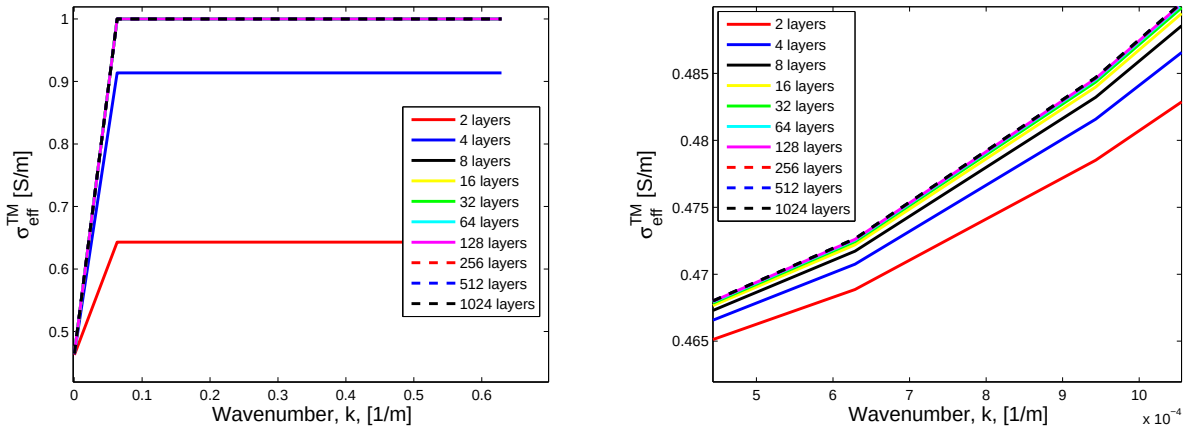

(a) (b)

Figure 3-10: (a) Effective TM isotropic conductivity (σ_{eff}^{TM}) for different number of layers with conductivity distributions (0.3 1) S/m, at f= 0.1 Hz when the reflection and transmission interactions are included. The zoom-in (b) shows $\sigma_{eff}^{TM} = \sigma_{eff}^{TE}$ only at $k \approx 0$.

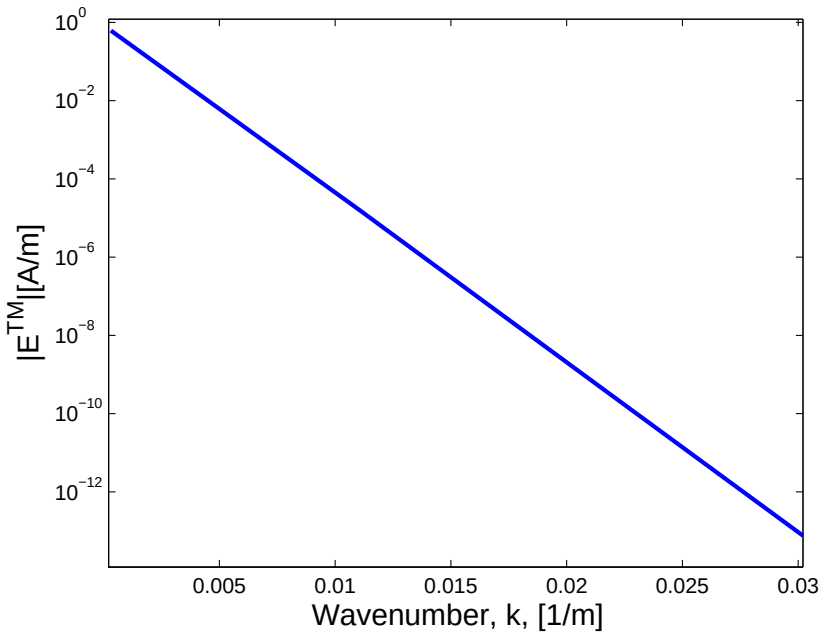

Figure 3-11: Absolute effective amplitude of TM electric field at relevant k values in the k-spectrum for 1 km thick layer at frequencies of 0.1 Hz for both all the different number of layers

3-1-5 Effective VTI medium for the isotropic layered earth: Model

The overburden (isotropic layered earth) of Figure 3-2 can be replaced with an effective anisotropic model with effective VTI parameters σ^v_{eff} and σ^h_{eff}. The total thickness, T of the overburden is held constant and the effective electric field is:

$$E^{TM}_{N+1} = \frac{(1+R_{eff})(1+R_0)\exp(-\Gamma_{eff}T)}{(1+R_{eff}\exp(-2\Gamma_{eff}T))}, \tag{3-24}$$

where

$$R_0 = \frac{r_0 + R_{eff}\exp(-2\Gamma_{eff}T)}{1+r_0R_{eff}\exp(-2\Gamma_{eff}T)}, \tag{3-25}$$

$$r_0 = \frac{\sigma_{N+1}\Gamma_0 - \sigma_0\Gamma_{eff}}{\sigma_{N+1}\Gamma_0 + \sigma_0\Gamma_{eff}} = 1, \tag{3-26}$$

$$r_{eff} = \frac{\sigma_{N+1}\Gamma_{eff} - \sigma^h_{eff}\Gamma_{N+1}}{\sigma_{N+1}\Gamma_{eff} + \sigma^h_{eff}\Gamma_{N+1}}, \tag{3-27}$$

$$\Gamma_{eff} = \sqrt{\frac{\sigma^h_{eff}}{\sigma^v_{eff}}k^2 + i\omega\mu\sigma^h_{eff}}, \tag{3-28}$$

$$\Gamma_{N+1} = \sqrt{k^2 + i\omega\mu\sigma_{N+1}} \tag{3-29}$$

where $R_{eff} = r_{eff}$; R_{eff} is the global TM reflection coefficient of the interface separating the effective medium in domain $\mathbb{D}_n$ and domain $\mathbb{D}_{N+1}$, r_{eff} is its local reflection coefficient; R_0 is the global TM reflection coefficient of the interface between domain $\mathbb{D}_0$ and effective medium domain $\mathbb{D}_n$, and r_0 is its local reflection coefficient; Γ_0 and Γ_{eff} are the TM vertical wavenumber for domains $\mathbb{D}_0$ and $\mathbb{D}_n$ respectively.

The effective VTI property of layered earth in Figure 3-4 are found by optimizing the error between equations (3-20) and (3-24). Effective VTI conductivities, for 2 layers at 10 Hz, are shown in Figure 3-12(a). These effective VTI conductivities fluctuate as the k changes. At very small magnitude of wavenumber the effective medium is anisotropic while at high wavenumber the medium becomes isotropic (Figure 3-12(b)). Similar solutions and fluctuations are found at all frequencies in the range of $(0.1 - 10)$ Hz.

3-1-6 Effective VTI medium of a VTI layered earth

In this subsection some anisotropy will be included in each of the layers in Figure 3-4. The conductivity contrast between layers will also be varied to quantify how much influence this has on the overall solution. The frequency of transmission is 0.1 Hz. Firstly, effective horizontal and vertical conductivities are inverted for a VTI layered earth with uniform anisotropic ratio ($\sigma_v/\sigma_h = 2.58$) in each layer. This set up is to model the shale formations as reported in the (Ellis *et al.*, 2010a). Figure 3-13(a) shows the plot of the solution.

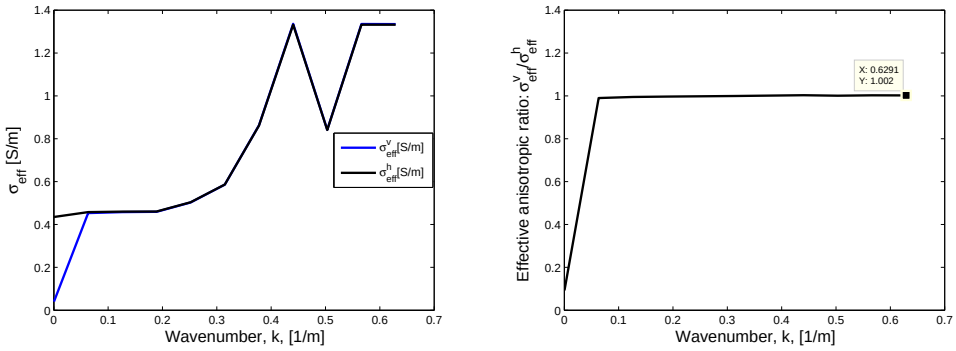

(a) (b)

Figure 3-12: (a) Effective VTI parameters and (b) effective VTI anisotropic ratio for horizontally stratified isotropic 2 layers at f= 10 Hz.

The effective parameters fluctuate highly at different wavenumber k (which may be due to the anisotropy) but the effective anisotropic ratio remains more or less constant at high wavenumber k. The value of the inverted anisotropic ratio approaches the value of average anisotropic ratio of 2.58, see Figure 3-13(b). Secondly, (0.3 0.35) S/m and (0.3 1) S/m conductivity distributions are alternated between layers and equal anisotropic ratio is included in each of these layers according to the published results in the (Ellis *et al.*, 2010a). The anisotropic ratio used is 2.58. Figure 3-14(a) to 3-14(d) show solution space plots of the effective VTI parameters for 2 and 1024 layers at 0.1 Hz for (0.3 0.35) S/m conductivity distribution. From these figures, it is established that the different effective solutions exist at different values of k, though the anisotropic ratio remains approximately constant, (2.58), at large k. Lastly, we re-distribute non-uniform anisotropy into adjacent layers according to the published data of (Ellis *et al.*, 2010a). The anisotropic ratio in odd and even layers are 2.58 and 3.23 respectively. Figure 3-15(a) further establishes that there is no existence of unique effective VTI conductivities even for large k. Moreover, the effective anisotropic ratio reduces as the wavenumber k increases, see Figure 3-15(b).

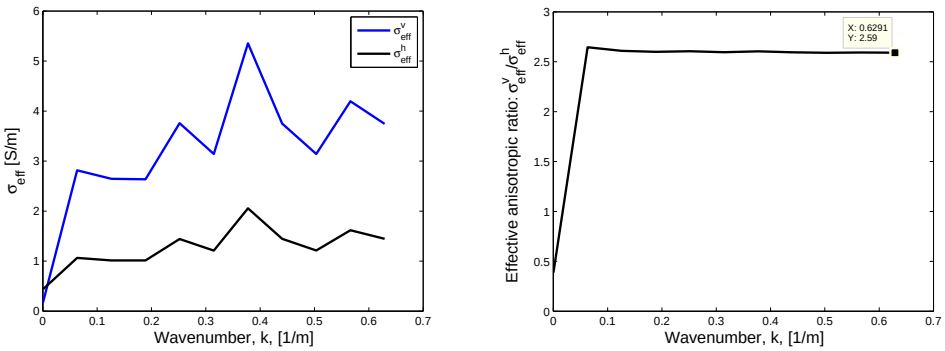

(a) (b)

Figure 3-13: (a) Inverted effective horizontal and vertical conductivities and (b) the effective anisotropic ratio for 2 layers with conductivity distribution of (0.3 0.35)S/m and a uniform anisotropic ratio distribution of $\sigma_v/\sigma_h = 2.58$ in each layer; the frequency of transmission is 0.1 Hz.

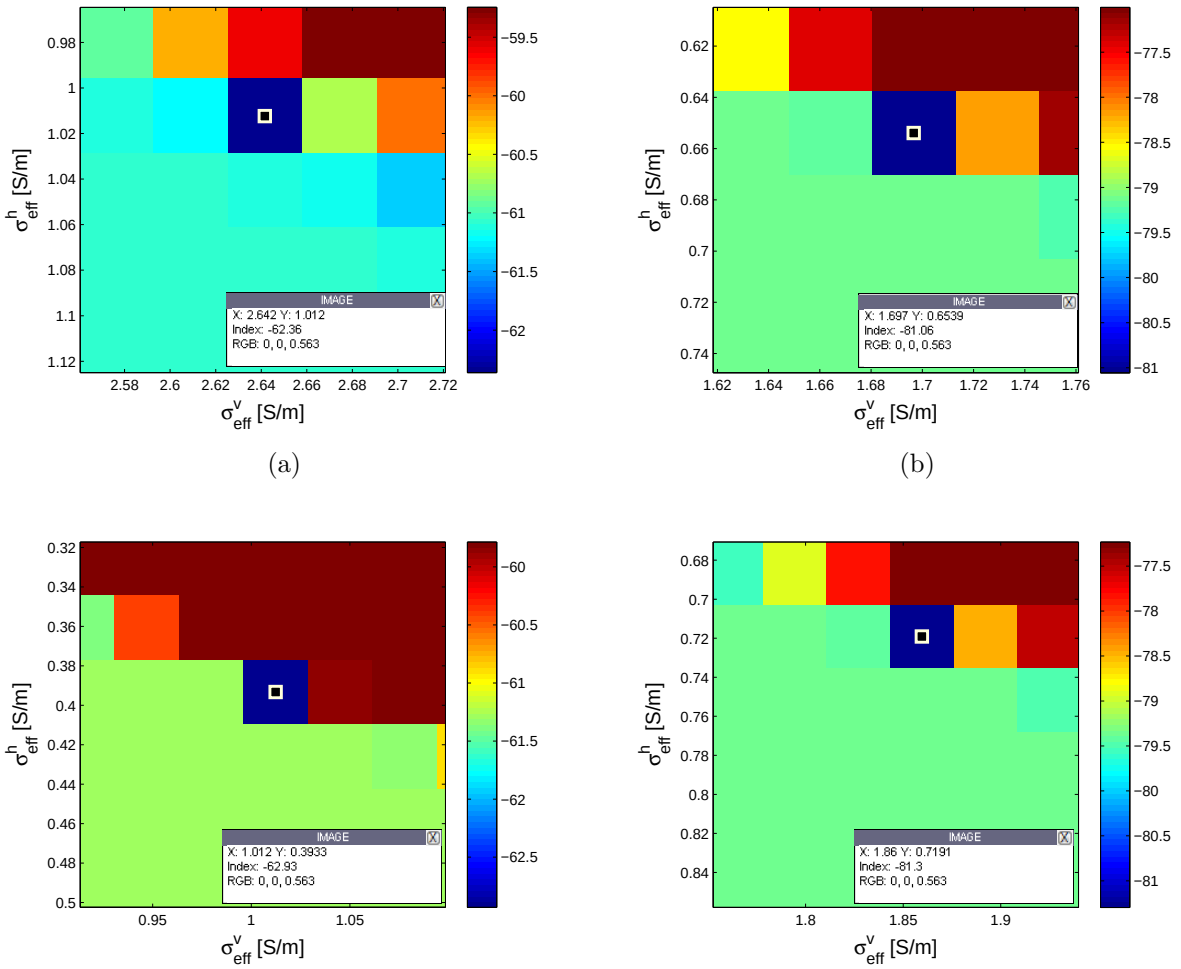

Figure 3-14: Solution space of objective function logarithm in σ^h_{eff} and σ^v_{eff} plane of VTI 2 and 1024 layered system with conductivity distribution $(0.3 \quad 0.35)\,\mathrm{S/m}$ in alternating layers. Solutions at 50% of k_{max} for (a) 2 and (c) 1024 layers differ from solutions at 60% of k_{max} for (b) 2 and (d) 1024 layers.

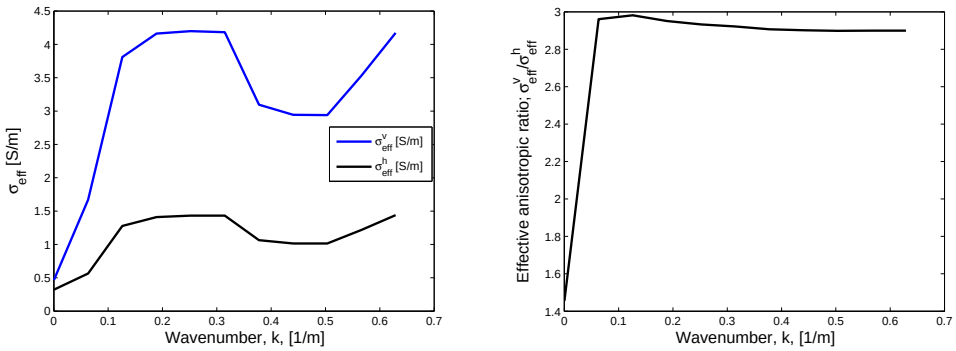

(a) (b)

Figure 3-15: (a) Inverted effective horizontal and vertical conductivities and (b) the effective anisotropic ratio for 2 layers with conductivity distribution of (0.3 0.35)S/m and with the inclusion of non-uniform anisotropic ratio of σ_v/σ_h of 2.58 and 3.23 in odd and even layer respectively; the frequency of transmission is 0.1 Hz.

Chapter 4

Effective TE and TM conductivities from horizontal electric field due to horizontal dipole source

In this chapter we invert for both effective TE conductivity and effective TM conductivity from the horizontal electric field due to horizontal electric dipole E_{xx}. This modeling is the same as the one done in chapter three but now with the consideration of orientation of the field. This is possible because from equation (1-42) it is seen that E_{xx} contains both TM-mode field (E_z) and TE-mode field (H_z) which is re-written here as:

$$E_{xx} = -\frac{ik_x}{\eta\kappa^2}\partial_z\eta^v E_{zx} + \frac{ik_y\zeta^v}{\kappa^2}H_{zx}, \tag{4-1}$$

In this section we use lower case Latin subscript to denote layer numbers and the depth -coordinate in space is now denoted as $z = x_3$ to avoid confusion of notation assignments. The layered earth considered is similar to the one in the preceding chapter with homogeneous upper domain $\mathbb{D}_0$ defined by $z < 0$; domain $\mathbb{D}_n$ which contains layers of finite thickness defined by $z_{n-1} < z < z_n$ for $n = 1, 2, 3, ..., N$ and the lower half space domain $\mathbb{D}_{N+1}$ defined by $z > z_{N+1}$. The source occupies the domain $\mathbb{D}_s$. For layers below the source layer, $s < n \leq N + 1$, the TM-mode electric field amplitude at $N + 1$ is given as:

$$E_{zx;N+1} = A^+_{N+1}W^d_n, \tag{4-2}$$

where the downgoing propagator inside each layer n is $W^d_n = \exp(-\Gamma_n(z - z_n))$ and the downgoing electric field at $N + 1$ layer is A^+_{N+1} and it is given by:

$$A^+_{N+1} = \frac{\eta^v_{s+1}}{\eta^v_{N+1}}A^+_{s+1}\prod_{m=s+2}^{N+1}\frac{(1 + R^+_{m-1})\exp(-\Gamma_{m-1}d_{m-1})}{1 + R^+_m\exp(-2\Gamma_m d_m)}, \tag{4-3}$$

and

$$\partial_z E_{zx;N+1} = -\Gamma_{N+1} A^+_{N+1} \exp(-\Gamma_{N+1}(z - z_n)), \tag{4-4}$$

The field just below the source layer is A^+_{s+1} and it is given by

$$A^+_{s+1} = \frac{\eta^v_s}{\eta^v_{s+1}} \frac{X^{TM}(z=0)(1+R^+_s)(1-R^-_s)\exp(-\Gamma_s d_s)}{1+(1-R^+_s R^-_s \exp(-2\Gamma_s d_s))\exp(-2\Gamma_{s+1} d_{s+1})}, \tag{4-5}$$

with source function $X^{TM} = \frac{ik_x}{2\eta^v_s}$, equation (4-5) becomes:

$$A^+_{s+1} = \frac{ik_x}{2\eta^v_{s+1}} \frac{(1+R^+_s)(1-R^-_s)\exp(-\Gamma_s d_s)}{(1-R^+_s R^-_s \exp(-2\Gamma_s d_s))\exp(-2\Gamma_{s+1} d_{s+1})}, \tag{4-6}$$

Putting equations (4-6) into (4-3) and then into (4-2) we have:

$$E^{TM} = \frac{(ik_x)^2}{2\eta_{N+1}\kappa^2} \Gamma_{N+1} \exp(-\Gamma_{N+1}(z - z_N)) \frac{(1+R^+_s)(1-R^-_s)\exp(-\Gamma_s d_s)}{(1-R^+_s R^-_s \exp(-2\Gamma_s d_s))\exp(-2\Gamma_{s+1} d_{s+1})} \prod_{m=s+2}^{N+1} \frac{(1+R^+_{m-1})\exp(-\Gamma_{m-1} d_{m-1})}{1+R^+_m \exp(-2\Gamma_m d_m)} \tag{4-7}$$

Equation (4-7) can also be written as:

$$E^{TM} = -\frac{(\cos(\varphi))^2}{2\sigma_{N+1}} \Gamma_{N+1} \frac{(1+R^+_s)(1-R^-_s)\exp(-\Gamma_s d_s)}{(1-R^+_s R^-_s \exp(-2\Gamma_s d_s))(1+R^+_{s+1}\exp(-2\Gamma_{s+1} d_{s+1}))} \prod_{m=s+2}^{N+1} \frac{(1+R^+_{m-1})\exp(-\Gamma_{m-1} d_{m-1})}{1+R^+_m \exp(-2\Gamma_m d_m)}, \tag{4-8}$$

where $k_x = \kappa\cos(\varphi)$, φ is the propagation angle between κ and k_x; the TM global reflection coefficient is recursively defined as:

$$R^\pm_n = \frac{r^\pm_n + R^\pm_{n\pm1}\exp(-2\Gamma_{n\pm1} d_{n\pm1})}{1 + r^\pm_n R^\pm_{n\pm1}\exp(-2\Gamma_{n\pm1} d_{n\pm1})}, \tag{4-9}$$

with the local reflection coefficients given as:

$$r^\pm_n = \frac{\eta_{n\pm1}\Gamma_n - \eta_n \Gamma_{n\pm1}}{\eta_{n\pm1}\Gamma_n + \eta_n \Gamma_{n\pm1}} \tag{4-10}$$

The TE-mode electric field (E^{TE}) is found in a similar way but with TE-mode source function (X^{TE}). Following the principle of equivalence: $\zeta = -\eta$; $J^e = -J^m$, X^{TE} can be written from X^{TM} as $X^{TE} = \frac{-ik_y}{2\Gamma^{TE}_s}$ and with this we have:

$$E^{TE} = \frac{(ik_y)^2}{2\bar{\Gamma}_s\kappa^2} \zeta_{N+1} \frac{\eta^v_s}{\eta^v_{N+1}} \exp(-\bar{\Gamma}_{N+1}(z - z_N)) \frac{(1+\bar{R}^+_s)(1+\bar{R}^-_s)\exp(-\bar{\Gamma}_s d_s)}{(1-\bar{R}^+_s\bar{R}^-_s)(1+\bar{R}^+_{s+1}\exp(-2\bar{\Gamma}_{s+1} d_{s+1}))} \prod_{m=s+2}^{N+1} \frac{(1+\bar{R}^+_{m-1})\exp(-\bar{\Gamma}_{m-1} d_{m-1})}{1+\bar{R}^+_m \exp(-2\bar{\Gamma}_m d_m)}, \tag{4-11}$$

Equation (4-11) can also be written as:

$$E^{TE} = -\frac{(\sin(\varphi))^2}{2\bar{\Gamma}_s}\zeta_s \frac{(1+\bar{R}_s^+)(1+\bar{R}_s^-)\exp(-\bar{\Gamma}_s d_s)}{(1-\bar{R}_s^+\bar{R}_s^-)(1+\bar{R}_{s+1}^+\exp(-2\bar{\Gamma}_{s+1}d_{s+1}))} \prod_{m=s+2}^{N+1} \frac{(1+\bar{R}_{m-1}^+)\exp(-\bar{\Gamma}_{m-1}d_{m-1})}{1+\bar{R}_m^+\exp(-2\bar{\Gamma}_m d_m)}, \tag{4-12}$$

where $k_y = \kappa\sin(\varphi)$, φ is the propagation angle between κ and k_x; the TE global reflection coefficient is recursively defined as:

$$\bar{R}_n^{\pm} = \frac{\bar{r}_n^{\pm} + \bar{R}_{n\pm1}^{\pm}\exp(-2\bar{\Gamma}_{n\pm1}d_{n\pm1})}{1+\bar{r}_n^{\pm}\bar{R}_{n\pm1}^{\pm}\exp(-2\bar{\Gamma}_{n\pm1}d_{n\pm1})}, \tag{4-13}$$

with the local reflection coefficients is given as:

$$\bar{r}_n^{\pm} = \frac{\zeta_{n\pm1}\bar{\Gamma}_n - \zeta_n\bar{\Gamma}_{n\pm1}}{\zeta_{n\pm1}\bar{\Gamma}_n + \zeta_n\bar{\Gamma}_{n\pm1}} \tag{4-14}$$

For an effective medium, the effective TM and TE electric amplitudes are:

$$E_{eff}^{TM} = -\frac{(\cos(\varphi))^2}{2\sigma_{N+1}}\Gamma_{N+1}\frac{(1+R_{eff}^+)(1-R_{eff}^-)\exp(-\Gamma_s d_s)}{1-R_{eff}^+R_{eff}^-\exp\left(-2\Gamma_{eff}T\right)}, \tag{4-15}$$

$$E_{eff}^{TE} = -\frac{(\sin(\varphi))^2}{2\bar{\Gamma}_s}\zeta_s\frac{(1+\bar{R}_{eff}^+)(1+\bar{R}_{eff}^-)\exp(-\bar{\Gamma}_s d_s)}{1-\bar{R}_{eff}^+\bar{R}_{eff}^-\exp\left(-2\bar{\Gamma}_{eff}T\right)}, \tag{4-16}$$

where $R_{eff} = R_s$ and $\Gamma_s = \Gamma_{eff}$ have been used for the effective medium to avoid mix-up of terms with the layered earth and $R_{N+1} = \bar{R}_{N+1} = 0$.

The error between the data and the model is minimized to find unique effective TE (σ_{eff}^{TE}) and TM (σ_{eff}^{TM}) conductivities but there is no existence of such unique solutions. Several local minima exist for different pairs of TE and TM conductivities. It is worth noting that in chapter three that the unique values were found for the individual (σ_{eff}^{TE}) and (σ_{eff}^{TM}) when the two modes were separated. The reason for the directional influence on finding unique (σ_{eff}^{TE}) and TM (σ_{eff}^{TM}) is not investigated in this report but would be an interesting research work to do.

Chapter 5

Conclusion

In an attempt to quantify the degree of anisotropy caused by layering in sediments Ellis *et al.* (2010a) adopted the 'moving window average method' to find the bulk vertical and horizontal resistivities of some resistivity logs from undeviated wells. They used equations (2-1) and (2-2) for calculating the bulk vertical and horizontal resistivities respectively within a window height of T (20-200 m); where conductivity of each layer is the inverse of resistivity. The ratio of the bulk vertical and bulk horizontal resistivity is the bulk anisotropic ratio.

To validate the published results of Ellis *et al.* (2010a), we have used the controlled source electromagnetic (CSEM) method, in the horizontal wavenumber-frequency domain ($k-\omega$), to investigate the effective medium theory for horizontally layered isotropic and vertically transverse isotropic (VTI) layered earth. It has been shown in this report that although there exists an effective isotropic conductivity for isotropic layered earth with or without the reflection and transmission interactions between layers, there are no effective VTI conductivities for horizontally layered isotropic and VTI layered earth.

Without reflection and transmission interactions, the homogenization of the layered earth is controlled by the magnitude of wavenumber, k over that of the diffusion constant of the vertical wavenumber, Γ. For small wavenumber, k, the effective conductivity is a function of square root of conductivity of each layer. At about 0.5% of the maximum wavenumber k_{max}, the dominance of k results in the homogenization of the layered system and therefore the effective isotropic conductivity becomes a fractional average of the layers conductivities, irrespective of the unit thickness of the layers. Thus anisotropy exists for small k and isotropy exists at large magnitude of wavenumber, k ($k = 0.5\%$ of k_{max}) because the diffusion constant of the vertical wavenumber, Γ is negligible. With the inclusion of reflection and transmission interactions in the layered system, effective isotropic conductivity exists only for very thin layering, where the effective skin depth or wavelength is large compared to the unit thickness in a layered system. Under these conditions, these

results are in good agreement with the 'moving window average method' of (Ellis *et al.*, 2010a) for finding only the bulk horizontal resistivity of resistivity logs from undeviated wells. It is important to know that effective isotropic TM and effective isotropic TE are equal only at very small magnitude of wavenumber, k but at large k the solutions are quite different due to the different limits of their reflection coefficients.

However, our numerical results show that the inverted effective VTI conductivities for horizontally layered isotropic and VTI layered earth are not stable within the range of wavenumber k. The solutions are k-dependent with different values at different wavenumber, k. The effective anisotropic ratio is also influenced by the conductivity contrasts between adjacent layers and the magnitude of anisotropy in each of the layers. From these results and observations, it implies that the 'moving window average method' adopted by Ellis *et al.* (2010a) is not a valid approach for modeling a layered earth, though it may be valid for a local measurement.

.

References

Adepelumi, A.A., & Falebita, D.E. 2011. Modeling improves Niger Delta CSEM results: Integration with logs, seismic data increases confidence. *A paper given at the Offshore West Africa Conference in Abuja, Nigeria.*

Backus, G.E. 1962. Long-wave elastic anisotropy produced by horizontal layering. *Journal of Geophysical Research*, **67**, 4427–4440.

Chave, A.D., & Cox, C. 1982. Controlled electromagnetic sources for measuring electrical conductivity beneath the oceans 1. Forward problem and model study. *Journal of Geophysical Research*, **87**, 5327–5338.

Choy, T.C. 1999. Effective Medium Theory-Principles and Applications. *Oxford University Press, Oxford.*

Constable, S. 2010. Ten years of marine CSEM for hydrocarbon exploration. *Geophysics*, **75**, 75A67–75A81.

de Hoop, A.T. 1995. Handbook of Radiation and Scattering of Waves. *Academic Press, London.*

Eidesmo, T., Ellingsrud, S., MacGregor, L.M., Constable, S., Sinha, M.C., Johansen, S., Kong, F.N., & Westerdahl, H. 2002. Sea bed logging (SBL), a new method for remote and direct identification of hydrocarbon filled layers in deepwater areas. *first break*, **20**.

Ellingsrud, S., Eidesmo, T., Johansen, S., Sinha, M.C., MacGregor, L.M., & Constable, S. 2002. Remote sensing of hydrocarbon layers by seabed logging (SBL): Results from a cruise offshore Angola. *The Leading Edge.*

Ellis, M., Sinha, M., & Parr, R. 2010a. Role of fine-scale layering and grain alignment in the electrical anisotropy of marine sediment. *First Break*, **28**, 49–57.

Ellis, M. H., Sinha, M. C., Minshull, T. A., Sothcott, J., & Best, A. I. 2010b. An anisotropic model for the electrical resistivity of two-phase geologic materials. *Geophysics*, **75**, E161–E170.

Hashin, Z., & Shtrikman, S. 1962. A variational approach to the theory of the effective magnetic permeability of multiphase materials. *Journal of Applied Physics*, **33**, 3125–3131.

Hoversten, G. M., Newman, G. A., Geier, N., & Flanagan, G. 2006. 3D modeling of a deepwater EM exploration survey. *Geophysics*, **71**, G239–G248.

Ikelle, L.T., & Amundsen, L. 2005. Introduction to petroleum seismology. *Society of Exploration Geophysics*.

Kong, J.A. 1972. Electromagnetic fields due to dipole antennas over stratified anisotropic media. *Geophysics*, **37**, 985–996.

Løseth, L.O., Pedersen, H.M., Ursin, B., Amundsen, L., & Ellingsrud, S. 2006. Low-frequency electromagnetic fields in applied geophysics: Waves or diffusion? *Geophysics*, **71**, W29–W40.

Løseth, L.O., Pedersen, H.M., Schaug-Pettersen, T., Ellingsrud, S., & Eidesmo, T. 2008. A scaled experiment for the verification of the SeaBed logging method. *Journal of Applied Geophysics*, **64**, 47–55.

Maldovan, M., Bockstaller, M. R., Thomas, E.L., & Carter, W.C. 2003. Validation of the effective-medium approximation for the dielectric permittivity of oriented nanoparticle-filled materials: effective permittivity for dielectric nanoparticles in multilayer photonic composites. *Applied Physics B*, **76**, 877–884.

Mavko, G., Mukerji, T., & Dvorkin, J. 2003. The rock physics handbook: Tools for seismic analysis in porous media. *Cambridge University Press*.

Norris, A.N. 1985. A differential scheme for the effective moduli of composites. *Mechanics of Materials*, **4**, 1–16.

Sen, M., & Stoffa, P.L. 1995. Global Optimization Methods in Geophysical Inversion. *Elsevier, Amsterdam, The Netherlands*.

Sheng, P. 1990. Effective medium theory of sedimentary rocks. *Physical Review B*, **41**, 4508–4512.

Slob, E., Hunziker, J., & Mulder, W. A. 2010. Green's tensor for the diffusive electric field in a VTI half-space. *Progress In Electromagnetic Research*, **107**, 1–20.

Slob, E., Thorbecke, J., Hunziker, J., & Shoemaker, C. 2011. The electromagnetic response in a layered VTI medium: A new look at an old problem. *Unpublished*.

Um, E.S., & Alumbaugh, D.L. 2007. Special section-Marine controlled-source electromagnetic methods On the physics of the marine controlled-source electromagnetic method. *Geophysics*, **72**, WA13–WA26.

Zimmerman, R.W. 1991. Elastic moduli of a solid containing spherical inclusions. *Mechanics of Materials*, **12**, 17–24.